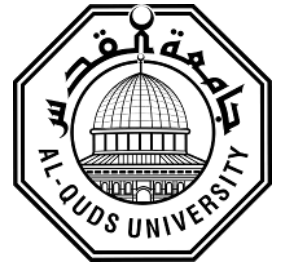


Deanship of Graduation Studies

Al-Quds University



Design and Simulation of a Novel Mutual Coupled Folded-dipole UHF RFID Tag Antenna for Metallic Objects

Dalia Zaher Tawfiq Mansour

M.Sc. Thesis

Jerusalem-Palestine

Jerusalem – Palestine
**Design and Simulation of a Novel Mutual Coupled Folded-
dipole UHF RFID Tag Antenna for Metallic Objects**

Prepared By:

Dalia Zaher Tawfiq Mansour

B.Sc.: Communication Engineering,
Technical University-PTUK, Palestine

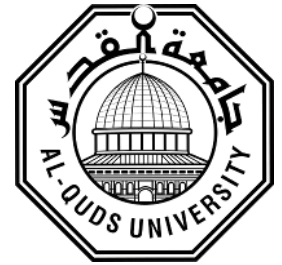
Supervisor: Dr. Mohammad Kouali

A thesis Submitted in Partial Fulfillment of the
Requirements for the Degree of Master of Electronic and
Computer Engineering, Faculty of Engineering at Al-Quds
University

Al-Quds University

Deanship of Graduation Studies

Electronic and Computer Engineering



Thesis Approval

**Design and Simulation of a Novel Mutual Coupled Folded-dipole
UHF RFID Tag Antenna for Metallic Objects**

Prepared By: Dalia Zaher Tawfiq Mansour

Registration No.: 21720387

Supervisor: Dr. Mohammad Kouali

Master thesis submitted and accepted, Date: 14 / 08 /2021

**The names and signatures of the examining committee
members are as follows:**

1- Head of Committee: Dr. Mohammad Kouali

2 -Internal Examiner: Dr. Ahmad Qutob

3 -External Examiner: Dr. Arafat Shabaneh

Signature

Signature

Signature

Three rectangular boxes containing handwritten signatures. The first box contains the signature 'Kouali'. The second box contains the signature 'Ahmad Qutob'. The third box contains the signature 'Arafat Shabaneh' and the date '30/8/2021' written below it.

Jerusalem – Palestine

Declaration:

I Certify that this thesis submitted for the Degree of Master is the result of my own research, except where otherwise acknowledged, and that this thesis (or any part of the same) has not been submitted for a higher degree to any other university or institution.

Signed by:**Dalia Mansour****Date: 14/08/2021**

Dedication

I dedicate this work to my great parents

Dalia Mansour

Acknowledgement

My work would never have been possible without Allah and the help of many people during my research. I would like to give special thanks to my supervisor for this project, Dr. Mohammad Koali, for his guidance, support and encouragement through my last two semesters.

Special thanks are also extended to Dr. Arafat Shabaneh and Dr. Fuad Erman for their help, suggestions and advice on my research work.

Last but not least, deeply thanks and appreciation to my father and mother for their infinite giving, support and encouragement. I would like also to thank my dear brothers Khalid, Mansour and Youssef.

ABSTRACT

Recently, radio frequency identification (RFID) technology has rapidly grown in various applications especially in supply chains. Such applications require a large number of tags placed on different object materials including metallic ones which increases the RFID challenges. The presence of metallic surfaces causes performance degradation of the RFID tag antenna. Thus, the demand for compact, low cost and high-gain tag antennas that work effectively on metals is increased.

In this work, a novel miniature mutual coupled folded-dipole metal mountable ultra-high frequency (UHF) RFID tag antenna is presented. The proposed RFID tag antenna is composed of two outer strips each loaded with seven identical open stubs and a middle shorter one forming two symmetrical nested combs. The two nested combs are connected at the center by the RFID chip which is attached to the two middle wide open stubs. Tuning the open stubs dimensions and the gaps between them provides a simple and flexible tuning mechanism to achieve an optimal impedance matching between the tag antenna and the IC chip at the required operating frequency band. Indeed, providing the mutual coupling effect between the open stubs increased the surface current thus, enhances the radiation field. The effect of the open stubs is investigated by increasing the open stubs number from three to seven at each outer strip. The proposed structure has a geometrical dimension of $55.8 \times 44 \times 1.5 \text{ mm}^3$ is implemented on a low cost dielectric Polytetrafluoroethylene (PTFE) substrate. The substrate is coated by a thin copper layer at the bottom side to be placed directly on metallic objects without the requirement of any spacer such as air or foam. The design is simulated by using CST microwave studio software. The realized gain of the tag antenna in free space is -7.13 dB. Placing the proposed tag antenna on a $20 \times 20 \text{ cm}^2$ metallic plate enhanced its realized gain by 3.57 dB compared to free space at a resonance

frequency of 912 MHz. The computed detection distance achieved 11.1 m when the tag is mounted on the 20× 20 cm² metallic plate and 7.37 m in free space with the estimation of using 4 W EIRP. The proposed tag antenna has a directivity of 3.24 dB in free space. The directivity increased to 7.36 dB when the tag is mounted on the metallic plate. The effect of varying the dimensions of the metallic plate is studied. The same read range of 11.1 m is achieved by varying the length of the metallic plate from 20 cm to 10 cm with a fixed width of 20 cm. On the other hand, the read range decreased to 7.81 m when the metallic plate width is decreased from 20 cm to 10 cm with a fixed length of 20 cm. In addition, the proposed tag antenna was placed on three different 20× 20 cm² dielectric plates. The simulated realized gain is -8.63 dB and the computed detection distance is 6.51 m when the presented tag is placed on paper. Moreover, the computed detection distance of the proposed tag antenna is 6.29 m and 5.94 m when the proposed tag is placed on 20× 20 cm² polycarbonate and glass plate respectively. The presented tag antenna is implemented to operate at the North American band (902 -928 MHz). The tag structure is simple and inexpensive, whereby it has no shorting elements or metallic via. The presented design does not require any complex fabrication work. Moreover, the proposed RFID tag is compact and has sufficient gain to achieve a relatively high read range. Thus, the proposed tag can be used for various RFID applications.

TABLE OF CONTENTS

Declaration	I
Dedication	II
Acknowledgement	III
Abstract	
IV	
Table of Contents	
VI	
List of Figures	IX
List of Tables	XII
List of Acronyms	XIII
CHAPTER 1 INTRODUCTION	1
1.1 Motivation and Problem Statement	2
1.2 Literature Review	3
1.3 Research Aim and Objectives	6
1.4 Thesis Contribution	7
1.5 Thesis Organization	7
CHAPTER 2 BACKGROUND	9
2.1 Introduction to RFID	10
2.2 Brief History	11
2.3 RFID Systems Types and Regulations	13
2.3.1 Passive UHF RFID Systems Regulations	16
2.4 RFID System Components	18
2.4.1 RFID Tags	18
2.4.2 RFID Readers	20
2.4.3 RFID Antennas	22
2.5 RFID UHF Tag Antenna Design Considerations	22

2.5.1 Antenna Shape and Size	22
2.5.2 Bandwidth.....	23
2.5.3 Radiation Pattern	24
2.5.4 Directivity and Gain	25
2.5.5 Impedance Matching	27
2.5.6 Read Range.....	30
2.5.7 Fabrication Material and Process	31
2.5.8 Proximity to Object	31
2.6 RFID Applications	31
CHAPTER 3 PASSIVE UHF RFID TAG ANTENNA	34
3.1 Impedance Matching Techniques for UHF Tag Antennas	35
3.1.1 T-Match Method.....	35
3.1.2 Inductively-Coupled Method.....	36
3.1.3 Nested-Slot Method.....	38
3.1.4 Open Stubs Method.....	39
3.2 Folded Dipole Antenna	41
3.3 Effect of Metal on UHF RFID Tag.....	44
3.4 Passive UHF RFID Tag Antennas for Metallic Objects.....	47
3.5 Scope of Research.....	48
3.6 Design Methodology.....	50
CHAPTER 4 A NOVEL MUTUALLY COUPLED FOLDED DIPOLE UHF RFID TAG ANTENNA	53
4.1 Design and Simulation Process.....	54
4.1.1 Simulation Using CST Software	54
4.1.2 Higgs 4 chip.....	56
4.1.3 Initial Antenna Structure	56
4.2 Final Antenna Structure	61
4.3 The Open Stubs Effect	62
4.4 Parametric Study	65

CHAPTER 5 SIMULATION RESULTS AND DISCUSSION	69
5.1 Simulation Results	70
5.1.1 Reflection Coefficient S_{11} and VSWR	70
5.1.2 Radiation Pattern	72
5.1.3 Gain and Directivity	73
5.1.4 Realized Gain	74
5.1.5 Read Range	75
5.2 Study of Back Metallic Object Effect.....	75
5.3 The Proposed RFID Tag Antenna Mounted on Non-Metallic Objects.....	78
5.4 Performance Comparison.....	81
CHAPTER 6 CONCLUSION AND FUTURE WORK	85
6.1 Conclusion	86
6.2 Future Work	87
References	89
Appendix A	97

List of Figures

List of Figures	Page No
Figure 2.1 Typical RFID system [15].	11
Figure 2.2 Inductive coupling RFID system.	15
Figure 2.3 Backscatter RFID system [4], [22].	16
Figure 2.4 UHF RFID frequency bands around the world [26].	17
Figure 2.5 Passive RFID tag components [28].	18
Figure 2.6 Types of RFID tags [29].	19
Figure 2.7 RFID reader types [32].	21
Figure 2.8 Different antenna radiation patterns [37].	24
Figure 2.9 Antenna field regions.	25
Figure 2.10 Simplified block diagram and equivalent circuit of a passive RFID tag [40].	28
Figure 3.1 The T-match configuration and its equivalent circuit.	36
Figure 3.2 Loop inductively-coupled method and its equivalent circuit.	37
Figure 3.3 A U-shaped inductively coupled feed coplanar tag antenna.	38
Figure 3.4 The nested-slot configuration and its equivalent circuit.	39
Figure 3.5 A slotted circular patch loaded with open stubs.	40
Figure 3.6 A half-wavelength dipole (a) structure [48] and (b) radiation pattern [36].	42
Figure 3.7 A folded dipole structure.	43
Figure 3.8 Simple illustration of the boundary conditions where (a) electric fields and (b) magnetic fields near a metallic surface.	46
Figure 3.9 Methodology design flow of RFID tag antennas.	51
Figure 4.1 Configuration of the initial proposed tag antenna.	58
Figure 4.2 Simulated reflection coefficient response of the initial antenna structure at different L values.	59
Figure 4.3 Simulated reflection coefficient response of the initial antenna structure with additional open stubs and the simulated reflection coefficient of the final structure.	60

Figure 4.4 Configuration of the proposed tag antenna.	61
Figure 4.5 Input impedance of the tag antenna at (a) first stage with three segments, second stage with five segments and (b) final stage with seven segments.	63
Figure 4.6 Tag antenna's surface current distribution at the resonance frequency for each design stage; (a) first stage, (b) second stage and (c) final stage.	64
Figure 4.7 Simulated reflection coefficient response at different L values.	66
Figure 4.8 Simulated reflection coefficient response at different W_1 values.	66
Figure 4.9 Simulated reflection coefficient response at different A values.	67
Figure 4.10 Simulated reflection coefficient response at different S values.	67
Figure 4.11 Simulated reflection coefficient response at different S_1 values.	68
Figure 5.1 S-parameter of the proposed tag antenna.	71
Figure 5.2 VSWR of the proposed RFID tag antenna over UHF band.	71
Figure 5.3 Radiation pattern of the RFID tag antenna at the resonance frequency 912 MHz (a) polar radiation pattern (b) 3D radiation pattern.	72
Figure 5.4 Simulated gain of the presented RFID tag antenna placed on 200×200 mm ² metal plate and in free space.	73
Figure 5.5 The directivity of the proposed RFID tag antenna placed on 200×200 mm ² metal plate and at free space.	74
Figure 5.6 The realized gain of the proposed tag antenna.	74
Figure 5.7 Simulated realized gain of the proposed tag antenna for the metal plate with different (a) plate length L_y and (b) plate width W_x	76
Figure 5.8 The radiation pattern of the presented tag antenna mounted on 20×10 cm ² (a) polar radiation pattern, (b) 3D radiation pattern.	78
Figure 5.9 The radiation pattern of the presented tag antenna mounted on 10×20 cm ² (a) polar radiation pattern, (b) 3D radiation pattern.	78
Figure 5.10 Simulated realized gain of the proposed tag antenna when it is placed on different dielectric 200×200 mm ² plates, metal plate and in free space.	79
Figure 5.11 Radiation pattern of the RFID tag antenna placed on 200×200 mm ² glass plate at its resonance frequency (a) polar radiation pattern (b) 3D radiation pattern.	80

Figure 5.12 Radiation pattern of the RFID tag antenna placed on $200 \times 200 \text{ mm}^2$ Polycarbonate plate at its resonance frequency (a) polar radiation pattern (b) 3D radiation pattern.	81
--	----

List of Tables

List of Tables	Page No
Table 2.1 RFID systems characteristics.	14
Table 2.2 Allocated frequency band for UHF RFID and maximum reader allowed power according to regulations [24].	17
Table 2.3 RFID passive, active and semi-passive tags comparison.	20
Table 2.4 EPC RFID classes.	21
Table 4.1 Dimensions of the initial proposed RFID tag antenna (mm).	58
Table 4.2 Dimensions of the proposed RFID tag antenna (mm).	62
Table 5.1 Simulated resonant frequency, realized gain and computed read range of the proposed tag antenna mounted on metal plate has fixed length ($L = 20$ cm) and varying width (W).	77
Table 5.2 Simulated resonant frequency, realized gain and computed read range of the proposed tag antenna mounted on 20×20 cm ² metallic and non-metallic plates.	80
Table 5.3 Comparison between the proposed tag and previous published UHF RFID metal mountable tags.	83

List of Acronyms

RFID	Radio Frequency Identification
UHF	Ultra-High Frequency
RF	Radio Frequency
CST	Computer Simulation Technology
DMS	Defected Microstrip Surface
IFF	Identify Friend or Foe
EAS	Electronic Article Surveillance
EPC	Electronic Product Code
ISO	International Organization for Standardization
LF	Low Frequency
HF	High Frequency
EIRP	Equivalent Isotropic Radiated Power
ERP	Equivalent Radiated Power
FHSS	Frequency Hopping Spread Spectrum
LBT	Listen Before Talk
PTC	Power Transmission Coefficient
PRC	Power Reflection Coefficient
RL	Return Loss
VSWR	Voltage Standing Wave Ratio
PTFE	Polytetrafluoroethylene
PEC	Perfect Electric Conductor
AMC	Artificial Magnetic Conductor
EBG	Electromagnetic Bandgap
PIFA	Planar Inverted-F Antenna

Chapter 1

Introduction

Chapter One

Introduction

This chapter introduces the purpose of this thesis. It presents the research motivations, problem statements, literature review, aim and objectives. Finally, the thesis organization is presented.

1.1 Motivation and Problem Statement

Radio frequency identification (RFID) is an automatic wireless identification technology. It is used in hundreds of mainstream applications such as theft prevention, inventory management, vehicles, people and animals tracking, locating and tracking activities of patients, huge and laborious manufacturing process management and much more. RFID system composed of three components which are tag or transponder, RFID reader and a central processing unit. The RFID tag stores the object' data in an IC chip. The RFID reader transmits electromagnetic waves through an antenna towards the tag to read the objects' data. The tag encodes the stored data into the received wave and scatters it back to the reader. Thereafter, the reader extracts and decodes the data. Finally, the reader sends the data to the central processing unit. The power transfer amount is determined by the reader and tag antennas. The antennas are the main part of the RFID system. In general, the reader antenna has no restrictions on its geometrical parameters such as small-size. On the other hand, designing the tag antenna is the critical part, where an optimal impedance matching between the tag antenna and the IC chip should be achieved to power up the chip and improves the tag performance [1]. The demand of ultra-high frequency (UHF) RFID tags is growing substantially especially the passive ones. The Passive tags are used widely in supply chain management, access point systems, security, transportation systems and much more. Such

applications require a large number of tags placed on different object materials. Thus, the demand of small size and low cost tag is increased. Although the RFID advantages in supply chain management, it faces many challenges due to the increment of RFID technology implementations.

The major RFID challenges are [2]:

- Performance degradation of the RFID tag antenna due to the presence of metals.
- RFID tags' cost.
- Small tags with low gain.
- Impedance matching between the tag antenna and the IC chip.

These challenges should be considered through the tag antenna design processes. Decreasing the antenna size increases the ohmic loss [3]. Therefore, maintaining a balance between the tag size and performance is a critical issue. This thesis aims to design a novel RFID tag antenna with low profile, high gain and sufficient read range. Moreover, the proposed tag antenna is easy to fabricate and works effectively for metallic object applications. The computer simulation technology (CST) simulator is used for implementing and simulating the proposed design. The tag antenna is designed to operate at UHF RFID North America band (902-928MHz) [4].

1.2 Literature Review

In order to understand the RFID tag antenna design especially for metallic objects, many published researches of UHF RFID passive tags were reviewed. Many articles discussed different RFID tag antenna configurations, impedance matching techniques, substrates, IC chips and ground planes. Recently, the folded dipole antenna is used very widely due to its simple structure and low cost. In order to minimize the tag size and reduce the resonance frequency, the folded dipole antenna is used with various impedance matching techniques such as connecting identical stubs to

a circular slotted patch [5], loading triangular stubs [6], embedded of extra arms and outer strip lines at a C-shaped resonator [7] and using U-shaped inductively coupled feed [8], [9], [10]. Moreover, various approaches are presented to avoid the metallic effect such as using foam [6] and air spacer [11], Electromagnetic Bandgap (EBG) ground plane [12] and using multiple dielectric substrates [9], [13].

- **Slotted Circular Patch with Multiple Loading Stubs for Platform Insensitive Tag [5]**

In this paper, a compact metal-mountable patch UHF tag antenna is presented. The antenna is composed of a circular patch with a rectangular slot at the middle. Four open stubs are loaded to the patch to reduce the tag resonance frequency. The IC chip is attached to the patch center. The design is fabricated on a RO4003C dielectric substrate coated with a copper layer at the bottom side. Adjusting the open stubs and the rectangular slot dimensions are used to tune the resonance frequency and achieve an optimal impedance matching between the tag antenna and the IC chip.

- **Design and Characterization of a Compact Single Layer Modified S-Shaped Tag Antenna for UHF-RFID Applications [6]**

A single layer S-shaped UHF RFID tag is implemented on a FR4 substrate. The antenna structure is composed of two outer strips connected at the center by the IC chip. Each strip is loaded by a triangular stub to achieve conjugate impedance matching between the tag antenna and the IC chip. The triangular stubs shifted down the resonance frequency to the required UHF band. A foam spacer with a 1 cm thickness is used to separate the tag and the back metallic plate.

- **Coplanar UHF RFID tag antenna with U-shaped inductively coupled feed for metallic applications [9]**

In this paper, a dual-layer coplanar UHF RFID tag antenna for metallic objects is implemented. Two Via-loaded symmetrical coplanar grounds are used with two different dielectric substrates. At the top layer, a U-shaped feeder is added to provide the inductive coupling effect to the antenna to achieve an optimal impedance matching with sufficient gain.

- **U-Shaped Inductively Coupled Feed UHF RFID Tag Antenna with Defected Microstrip Surface for Metal Objects [8]**

A metal-mountable UHF RFID tag is proposed. The tag antenna consists of two U-shaped feeders inductively coupled with two transmission lines attached to a defected microstrip surface (DMS). To form the DMS, a rectangular slot is etched. Tuning the feeders' dimensions provides a flexible impedance matching mechanism between the tag antenna and the IC chip. The implementation of the DMS enhanced the antenna performance by increasing the realized gain.

- **Patch-loaded Semicircular Dipolar Antenna for Metal-Mountable UHF RFID Tag Design [13]**

In this research paper, the proposed antenna structure is composed of multilayers. Two RO4003C dielectric substrates are used. The top layer is composed of a pair of semicircular dipolar patches with a horizontal slot at the center. The middle layer (between the substrates) is consisting of semicircular dipolar patches with a vertical slot. Two shorting stubs are used

to connect the middle layer with the ground plane. Rotating the top patch provided an effective method to tune the resonance frequency and the impedance of the tag antenna.

In this proposed work, a folded dipole UHF RFID tag antenna for metallic objects is designed. Two outer strips are connected at the center by the IC chip. Seven identical open stubs are added to each upper and lower side of the design. The resonance frequency of the proposed tag is tuned by adjusting the stubs' number and dimensions. The open stubs are placed to form U-shaped segments to provide the inductive coupling effect where a mutual coupling is formed between the nested stubs. This provides an effective method to achieve optimal impedance matching between the tag antenna and the IC chip with high gain thus, relatively high read range. In addition, the design was implemented on a single dielectric substrate without using any via holes or shorting elements. The proposed tag has a regular ground plane placed directly on the metallic plates without adding any spacer.

1.3 Research Aim and Objectives

The main goal of this thesis is to design a novel miniature UHF RFID tag antenna using a mutually coupled open stubs for metallic object applications and suitable for mass production.

The main objectives of this research are:

- 1- To design a new mutually coupled folded-dipole tag antenna for metallic objects.
- 2- To provide a simple frequency tuning mechanism without using any shorting elements or hard fabrication work.
- 3- To study the back object dimensions and material effect.

1.4 Thesis Contribution

In this work, a novel mutually coupled folded-dipole UHF RFID tag antenna for metallic objects is designed and simulated. A simple frequency tuning and impedance matching mechanism is used without using any shorting elements or complicated fabrication process which makes the proposed design suitable for mass production. Indeed, varying the back metallic object dimensions and material is investigated.

1.5 Thesis Organization

This thesis has six chapters summarized as follow:

Chapter one: Identifies the motivation and problem statement of this work. Besides, it introduces the literature review, the main research objectives, thesis contribution and organization.

Chapter two: Provides an overview of RFID technology. It presents the background with a brief history of RFID technology. Then, it introduces types of RFID systems, frequency regulations, some details about RFID system components and tag antenna design considerations. Finally, RFID system applications are included and presented.

Chapter three: Describes different impedance matching techniques used in RFID tag antenna design with a brief background of folded dipole antenna type which used in the proposed tag design. Furthermore, the metallic surface effect on the RFID tag antenna performance is discussed besides some solutions are suggested. Finally, it describes the methodology of designing passive UHF RFID tag antenna.

Chapter four: Elaborates on the design of a novel mutually coupled folded dipole UHF RFID tag antenna. It illustrates the antenna structure, design stages and parametric study in terms of reflection coefficient factor using the full wave electromagnetic simulator CST software.

Chapter five: Includes the simulation results of the proposed tag performance in terms of gain, radiation pattern, directivity, realized gain and computed read range. In addition, it presents the effect of varying the back metallic plate dimensions as well as material on the realized gain, radiation pattern and read range.

Chapter six: Contains the research conclusion followed by future work recommendations.

Chapter 2

Background

Chapter Two

Background

In this chapter, a background and a brief history of RFID technology are presented. RFID system operating principles, types, and frequency regulations are introduced, followed by an overview of the main RFID system components tags and readers. This thesis aims to design a UHF RFID tag antenna thus; passive tag antenna design considerations are discussed. Finally, various applications of RFID systems are presented.

2.1 Introduction to RFID

RFID technology is a wireless communication that provides automatic identification and data collecting about physical objects or humans without requiring a line of sight. Nowadays, RFID is used in hundreds of mainstream applications such as theft prevention, inventory management, vehicles, people and animals tracking, race timing, traffic prevention, locating and tracking activities of patients, huge and laborious manufacturing process management, goods identification and transportation payment. Therefore, reducing costs, high speed, reducing errors and staff shortage are strength points of RFID technology. Moreover, RFID has the ability to detect multiple items simultaneously with non-line of site which makes it replace barcodes. Consequently, RFID system includes two main parts divided into simple components which are tags or transponders at the object end, and more complex components called readers or interrogators on the other end terminal. The RFID tag is composed of an antenna and a chip that contains memory where the tag's ID and object's data are stored in. RFID readers produce

magnetic fields with high frequency through antennas to obtain tag recognition. Tags may be active tags (powered by a battery), passive tags (activated by the radio signal sent by the reader) or semi-passive tags. The tag retransmits the received signal loaded with the data stored in its chip. Then the reader extracts the data from the magnetic field signal and passes it to a host computer system via a communication interface, where the data are stored in a database and evaluated at a later time [1], [14]. Figure 2.1 shows a typical RFID system.

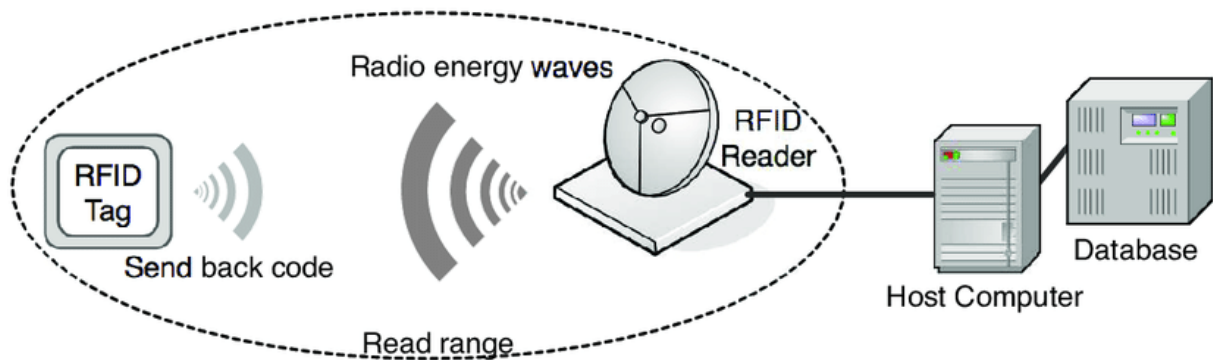


Figure 2.1 Typical RFID system [15].

2.2 Brief History

- In 1935, The “Identify Friend or Foe” system (IFF) was developed using radar by Sir Robert Alexander Watson-Watt. IFF is a long read range identification system; it was used in World War II to distinguish between friendly and enemy aircraft. Where a ground radar station sends a signal for identification, the friendly aircraft receives this signal and transmitted it back [16].

- In 1960s, the electronic article surveillance (EAS) system was developed for anti-theft and security purposes. EAS systems tags were only 1-bit tags (they have only two states “on” or “off”). Thus, the objects’ presence was detected without identifying them [17].
- In 1970s, the RFID explosion started to take place, where government laboratories, academic institutions and companies were working increasingly on RFID. Alfred Koelle, Steven Depp and Robert Freyman published an important development in a paper titled “Short-Range Radio-Telemetry for Electronic Identification Using Modulated Backscatter” [18]. The developments of RFID were applied for vehicle tracking, animal tracking and factory automation.
- In 1980s, full commercial RFID systems implementation started to extend in various applications include personal access systems, keyless entry, transportation applications and livestock management. The technology of CMOS integrated circuits was used with discrete components to build RFID tags. This produced tag size reduction and increased tags functionality.
- In 1990s, RFID started to enter the line of business and technology. In this decade, RFID began to be applied in vehicle toll collection and access control. Tags with CMOS circuits without discrete components were implemented [17].
- In 1999, in order to gather RFID researchers, manufacturers and users, the Auto-ID organization center at the Massachusetts Institute of Technology was established. This organization aimed to use RFID for identifying and tracking each object in the supply chain down to a certain level. To achieve this aim, the tag cost should be minimized. Therefore, each tag was labeled by a unique ID called (Electronic Product Code (EPC)). The EPC is related to the needed data about the object stored in the user database. Thus,

the tag chip required a memory enough only for the EPC instead of a huge data amount related to the object. By this concept the tag size was minimized thus, the cost was decreased.

- In 2003, Auto- ID center divided its work and responsibility into two organizations represented as Auto-ID labs and EPC global. EPC global and another organization called International Organization for Standardization (ISO) work on developing RFID standards [16].

2.3 RFID Systems Types and Regulations

The RFID system has several types which are classified based on their operating frequencies. These operation frequencies start from 125 KHz (low frequency LF) up to 2.45 GHz (microwave). RFID universal operation frequencies and their corresponding applications are classified in Table 2.1 [19], [20].

For the low frequency (LF) and the high frequency (HF), the near-field coupling principle is applied. The maximum detection distance of LF and HF RFID systems is limited as well as the low data rate transfer compares to the higher operating frequencies. Therefore, both LF and HF RFID systems are used for proximity applications only. However, the LF and HF are less sensitive to environmental changes, whereby the RFID tags of LF and HF systems are attached to objects containing liquids. On the other hand, the far-field radiation principle is employed for ultra-high frequency (UHF) and microwave operation frequencies. UHF has different frequency regulations in several countries around the world. Furthermore, UHF has anti-collision protocols, which provide the ability to read multiple tags simultaneously unlike LF and HF. UHF tags supply a larger memory size and better read range [21].

Table 2.1 RFID systems characteristics.

Type	Low Frequency LF	High Frequency HF	Ultra-High Frequency UHF	Microwave
Frequency Range	125-134 KHz	13.56 MHz	860- 960 MHz	2.4- 5.8 GHz
Tag expense	High	Medium, high	Medium	High
Reader Cost	Low	Medium	Medium, High	High
Read Range	30 cm	Up to 1 m	Up to 10 m	< 100 m
Data Rate	Low	Medium	High	High
Read Multiple Tags	Poor	Good	Very Good	Good
Application Fields	Animal identification, Access control, Security, Items with water identification	Smart cards, Access control, Ticketing, Item tracking, Libraries	Supply chain management, Container tracking, Item management, Toll collection	Location systems, Cars monitoring, Industry, Toll collection

The two main communication techniques used by RFID systems are:

- **Communication through coupling:**

Coupling means transferring energy between two different mediums, such as metallic wires or optical fibers. It has two common types: inductive (magnetic) coupling and capacitive (electrostatic) coupling. For inductive coupling, the energy transfers through a common magnetic field formed between two circuits due to mutual coupling between them. Inductive coupling is used by LF and HF RFID systems. Since the frequency of

these two systems is low which means a long wavelength, the convenient dipoles' length would be very long. Figure 2.2 shows the inductive coupling mechanism [4].

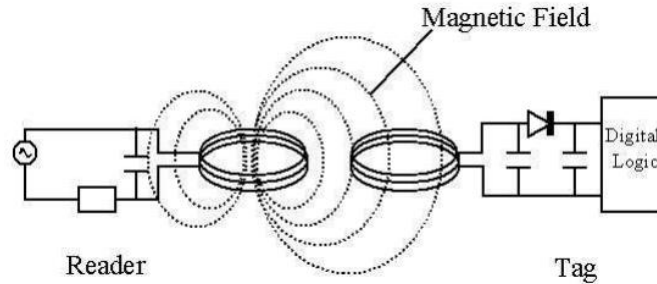


Figure 2.2 Inductive coupling RFID system.

- **Communication through back scattering:**

This mechanism based on collecting the received RF signals and reflecting them back to the sender. Figure 2.3 shows a backscatter RFID system. It is used in Passive UHF and microwave RFID systems. Hence, the RFID reader transmits electromagnetic waves to the RFID tag, the tag antenna receives the waves and power up the IC chip, then encodes the data into the received wave. Finally due to the charge device (capacitor) in the tag, the tag antenna scatters it back to the RFID reader.

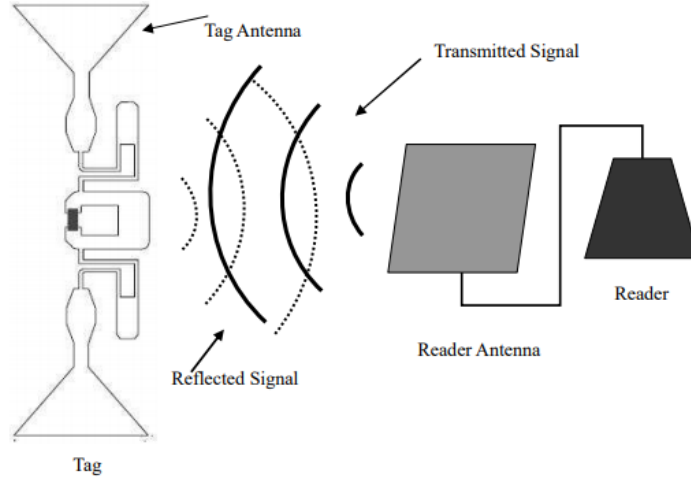


Figure 2.3 Backscatter RFID system [4], [22].

2.3.1 Passive UHF RFID Systems Regulations

Regulations refer to determine a specific available allocated frequency band and indicate the maximum allowable radiation power for the RFID application in a certain country. Thus, regulations are necessary to avoid interferences with any other devices. However, in this work the main focus is on passive UHF RFID tags. Therefore, passive UHF RFID system regulations are presented. Figure 2.4 shows the allowed frequency bands around the world. Regulations for other countries are found in [23] and [24]. The maximum allowable radiated power is expressed in terms of EIRP (equivalent isotropic radiated power) or ERP (equivalent radiated power). EIRP is the antenna radiated power expressed by the accepted power by the antenna and the antenna gain based on isotropic antenna. While ERP is the antenna radiated power expressed by the accepted power by the antenna and the antenna gain based on dipole antenna. The relation between EIRP and ERP is given by [25]:

$$P_{\text{EIRP}} = 1.64 \times P_{\text{ERP}} \quad (2.1)$$

Table 2.2 illustrates the regulated maximum radiated power for some countries.



Figure 2.4 UHF RFID frequency bands around the world [26].

Table 2.2 Allocated frequency band for UHF RFID and maximum reader allowed power according to regulations [24].

Country	Allocated Frequency Band	Maximum allowed radiated power
Australia	920- 926 MHz	4 W EIRP
United States	902- 928 MHz	4 W EIRP
United Kingdom	865.6-867.6 MHz	2 W ERP
China	920.5-924.5 MHz	2 W ERP
India	865-867 MHz	4 W EIRP

Moreover, regulations determine frequency channel selection techniques in a certain country. The most common frequency channel selection techniques are FHSS (Frequency Hopping Spread Spectrum) and LBT (Listen Before Talk) [27].

2.4 RFID System Components

A typical RFID system consists of three main components which are RFID tag, RFID reader, and a central processing unit. The main types and features of the RFID tags and readers are presented.

2.4.1 RFID Tags

Tags are made up of a small silicon chip and an antenna matched together on a dielectric substrate as shown in Figure 2.5. The microchip acts as a memory that contains a unique identification code that forms the tag's ID. Tags come in various shapes and sizes based on their type and RFID application [1]. Several tags are demonstrated in Figure 2.6. RFID Tags are divided into three types: active, passive and semi-passive.

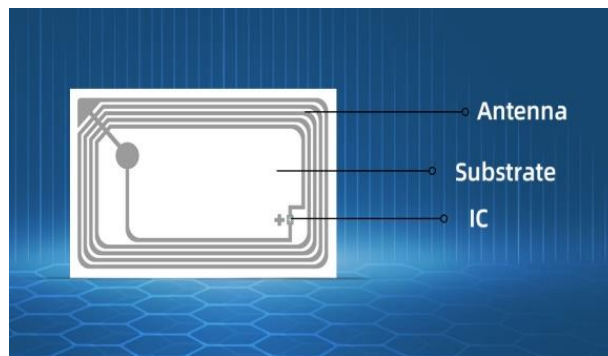


Figure 2.5 Passive RFID tag components [28].

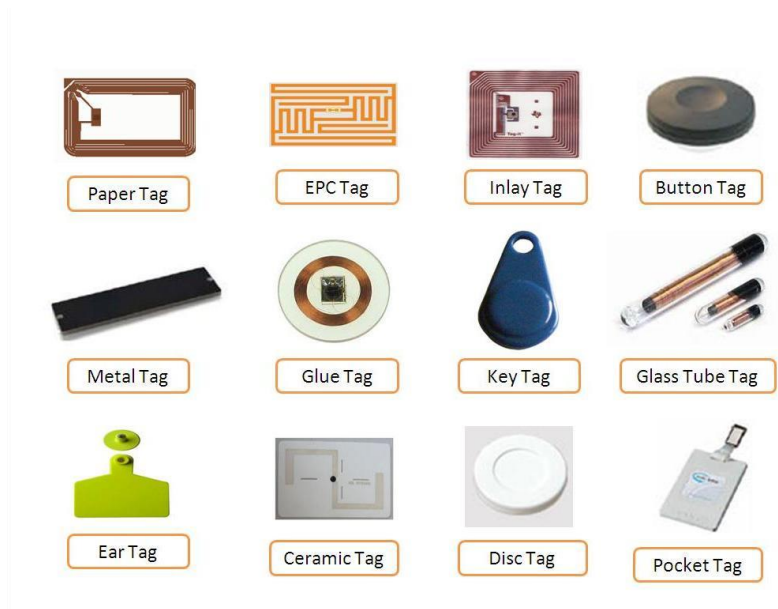


Figure 2.6 Types of RFID tags [29].

Active tags have their own power supply often a battery, which makes them able to send data directly to the reader rather than reflecting the energy received from it, which increases the read range. Active tags have various additional features including integrated sensors, increased memory and more logic. Because of the additional parts, active tags are more expensive and larger than passive tags. On the other hand, passive tags are completely powered by the incoming RF signal from the reader. Since passive tags have no batteries, the passive tags are much cheaper, smaller and have longer shelf life than active ones. Semi-passive tags are between passive and active tags. The semi-passive tags have a battery but are still powered by the reader's signals using the backscatter technique. In general, RFID tags types differ upon reading range, security, memory, type of the stored data, frequency and other characteristics. Table 2.3 shows a comparison between the three types of RFID tags. In addition, RFID tags are classified based on their capabilities such as read-write, read-only and extra data recordings like temperature or pressure.

Table 2.3 RFID passive, active and semi-passive tags comparison.

Tags and Features	Passive	Active	Semi –passive
Tag battery	No	Yes	Yes
Powered by backscattering of the reader	Yes	No	Yes
Size	Small	Big	Medium to large
Cost	Cheap	More expensive	less expensive
Range	3-5 meters	Up to 100 m	Up to 100 m
Potential shell life	Longer	Shorter	Longer

Compiled tags are classified into five classes listed in Table 2.4 [1], [30], [31].

2.4.2 RFID Readers

The RFID readers are considered the brain of the RFID system. RFID reader acts as a middleware between the RFID tag and the user application controller. RFID reader are called integrator; transmits and receives radio frequency RF waves in order to indicate the RFID tag then sends the tag information to the user software. The reader provides the required amount of energy to energize or activate passive and semi-passive tags at the reader’s electromagnetic field. However, Reaching the reader’s electromagnetic field is determined by the reader radiated power and the size of the tag and the reader antennas. Generally, the antenna size is determined based on the application requirements and the reader power is limited by the country regulations. RFID readers come in several types and shapes. As shown in Figure 2.7, RFID readers are fixed, handheld or mobile. Fixed readers are placed on desks, portals, walls or any stationary locations. On the other hand,

mobile readers are more flexible in reading tags at various locations since they are mounted on a forklift or other similar equipment [32], [33].

Table 2.4 EPC RFID classes.

Class	Definition	Description
Class 0	Read-only "passive tags"	Contains ID number that is written once by the manufacture
Class 1	Write once read many "passive tags"	Data can be written once by the user or the manufacture
Class 2	Read-Write "passive tags"	User can read and write data into the tags memory
Class 3	Read-write "semi-passive or active tags"	Contains sensors which record parameters like motion, temperature and pressure.
Class 4	Read write "active tags"	Has integrated transmitter these tags can contact with other tags and devices without the reader presence



Figure 2.7 RFID reader types [32].

2.4.3 RFID Antennas

RFID antennas are the middle-ware components for data communication between the reader and the tag and provide energy to passive tags. Antennas' shape and size differ based on their application requirements, whereby the antenna's design and placement play a main role in determining the coverage zone and communication accuracy. The tag antenna is fabricated with the tag chip on the substrate as a single unit. Since the IC chip is very tiny, with a total size less than 1 mm², the tag total size is typically determined by the antenna size and shape.

The readers' antenna is fabricated directly within the reader in the case of the handheld one. In other cases, several antennas are mounted away from the reader and strategically positioned to enhance the range and quality of the radio signals [4], [22].

2.5 RFID UHF Tag Antenna Design Considerations

The tag antenna is the main component of the RFID system. RFID tag antenna determines the amount of the transferred power, total tag size, tag cost and resonance frequency. Therefore, designing effective antennas is a critical issue. In this section, the main RFID tag antenna design considerations are discussed.

2.5.1 Antenna Shape and Size

In general, the larger antennas have higher gain where their ability to receive and reflect the readers' electromagnetic waves is stronger. However, large antennas have a higher cost and limit applications as they could be only placed on large objects. Thence, designing a compact-sized tag antenna compromised with gain is very desirable. In addition to the backed object size, the tag antenna size depends on the operation frequency wavelength. Typically, the tag antenna size is

approximately one-fourth wavelength of the lowest operation frequency. Tag antennas can be many shapes such as single dipole, folded dipole, C-shaped or spiral coil. When determining the shape of the tag antenna it should be simple, where its dimensions are easy to adjust in order to tune the antenna impedance without affecting the size much. Lastly, variation in the antenna design (size and shape) affects its behavior, operation frequency and properties [34].

2.5.2 Bandwidth

Antenna bandwidth is the range of frequencies in which the antenna operates effectively, means that the antenna performance parameters such as gain, input impedance, radiation pattern, and efficiency are met or get close to specific standard values. For dipole antenna, the bandwidth is a resonance frequency. The antenna bandwidth BW is defined as:

$$BW = f_U - f_L \quad (2.2)$$

where f_U and f_L are the upper and lower frequencies of the band respectively.

The bandwidth is usually expressed as a ratio or a percent. Fractional bandwidth B and percent bandwidth B_p are given by equations (2.3) and (2.4) respectively [35]:

$$B = \frac{BW}{f_c} \quad (2.3)$$

$$B_p = B \times 100 = \frac{BW}{f_c} \times 100 = 2 \left(\frac{f_U - f_L}{f_U + f_L} \right) \times 100 \quad (2.4)$$

where f_c is the center frequency [34]:

$$f_c = \frac{f_u + f_l}{2} \quad (2.5)$$

2.5.3 Radiation Pattern

The antenna radiation pattern is a graphical representation of the antenna radiation properties in the space in terms of directional coordinates. Where it illustrates the power radiated strength distribution around the antenna. Mostly, the radiation pattern is determined in the far-field region. The radiation pattern properties consist of field strength, radiation intensity, power flux density, polarization and directivity [36]. Different antenna types have different radiation patterns as shown in Figure 2.8.

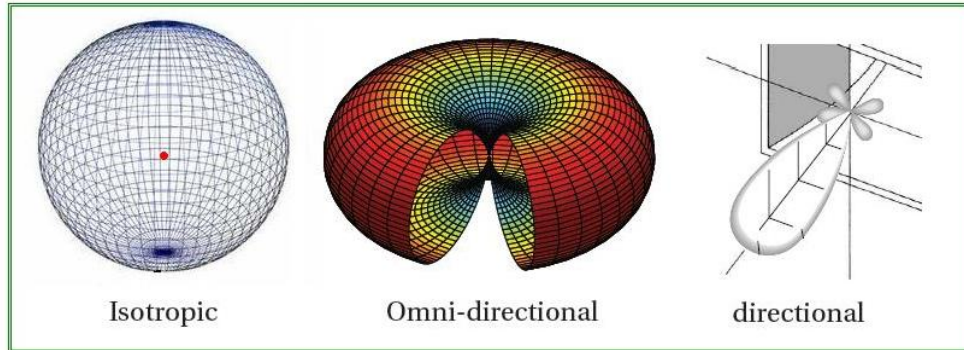


Figure 2.8 Different antenna radiation patterns [37].

The region surrounds the antenna is divided into three field regions as shown in Figure 2.9:

1. Reactive near-field: it is the region that directly surrounds the antenna where the reactive fields dominate. This region outer boundary is at a distance of:

$$R_1 = 0.62\sqrt{D^3/\lambda} \quad (2.6)$$

where R_1 is the distance away from the antenna surface, D is the antenna maximum dimension and λ is the wavelength.

2. Radiating near-field (Fresnel): this region locates between the reactive near field region and the far field region where the predominate fields here are the radiation fields. R_1 is the

inner boundary of this region and the outer boundary is at a distance R_2 away from the antenna surface:

$$R_2 = 2D^2 / \lambda \quad (2.7)$$

3. Far-field (Fraunhofer): it is the farthest region of the antenna surface where the radiation field distribution does not depend on the distance from the antenna. The far-field is located at distances further than $2D^2/\lambda$.

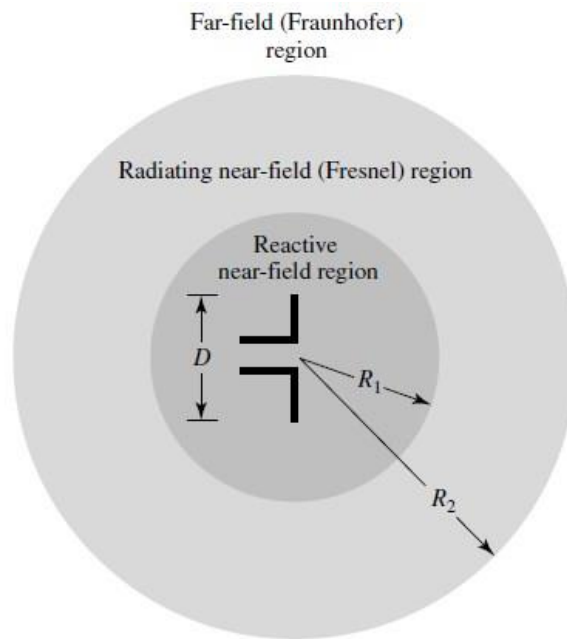


Figure 2.9 Antenna field regions.

The variation of the distance from the antenna (fields' boundaries) affects the phase and amplitude of the field pattern [36].

2.5.4 Directivity and Gain

The antenna's directivity is known as the ratio of the radiation intensity in a specific direction to the average radiation intensity in all directions, where the averaged radiation intensity equals the total radiated power from the antenna divided by 4π . If the direction is not determined, the direction

of maximum radiation intensity is estimated. In other expression, the directivity could be defined as the ratio of radiation intensity of a non-isotropic source to an isotropic source. Since the isotropic antenna has equal radiation intensity in all directions, its directivity is unity. The antenna directivity is given by [36]:

$$D = \frac{U}{U_0} = \frac{4\pi U}{P_{\text{rad}}} \quad (2.8)$$

Where D refers to the antenna's directivity, U is the radiation intensity of the test antenna, U_0 is the radiation intensity of an isotropic source and P_{rad} is the total power radiated by the antenna in Watt.

The antenna gain is one of the antenna performance parameters which describe the radiation ability of the antenna. The absolute antenna gain in a given direction is defined as the ratio of power density of the tested antenna radiated to a specific point at the far-field to the power density which would be radiated by an isotropic antenna at the same point [25]. It is given by:

$$G = \frac{4\pi r^2 W_{\text{rad}}}{4\pi r^2 W_{\text{rad}}^i} = \frac{W_{\text{rad}}}{W_{\text{rad}}^i} \quad (2.9)$$

where G is the antenna absolute gain, r is the distance between the antenna and the point at the far-field region where $r > 2D^2/\lambda$, W_{rad} is the radiation density of the tested antenna at the specified point and W_{rad}^i is the power density of the isotropic antenna. The antenna gain is closely related to the two factors: directivity and radiation efficiency. Subsequently, the antenna gain G is given in another form:

$$G = D \times e_r \quad (2.10)$$

where D is the directivity and e_r is the radiation efficiency. The gain is expressed by dB as G_{dBi} form which expressed as [25]:

$$G_{\text{dBi}} = 10\log_{10} \frac{W_{\text{rad}}}{W_{\text{rad}}^i} = 10\log_{10} G \quad (2.11)$$

The impedance mismatch between the tag antenna and IC chip loss is taken into account by the realized gain G_r . The realized gain is one of the most important parameters to evaluate the RFID tag antenna performance. The antenna realized gain is approximated as [38]:

$$G_r = G_a \times \tau \quad (2.12)$$

where G_a is the antenna gain and τ is the transmission coefficient.

2.5.5 Impedance Matching

Effective impedance matching between the passive RFID tag antenna and the IC chip is essential to retransmit the power delivered from the reader effectively. Whereby, tag antenna matching or mismatching with the microchip is directly related to the power absorption or reflection by the tag. RFID microchips are available at markets usually with low resistance real part at a range of 3 to 150 Ω and a high capacitive imaginary part at a range of -50 to -200 Ω . Since the impedance of the microchip is capacitive, the impedance of the tag antenna is tuned to be inductive to realize an efficient conjugate impedance matching. In general, using lumped elements to form an external matching network is inefficient since it increases the size and cost of the tag. Thence, the impedance matching should be achieved within the antenna structure design itself [39]. The tag antenna is directly connected to the chip as shown in Figure 2.10, where $Z_A = R_z + jX_a$ is the antenna complex impedance and $Z_C = R_c + jX_c$ refers to the chip complex impedance.

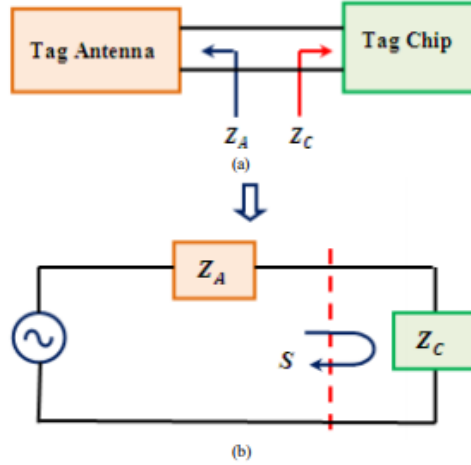


Figure 2.10 Simplified block diagram and equivalent circuit of a passive RFID tag [40].

The amount of power received by the tag from the reader (P_{tag}) is expressed by Friiss formula as:

$$P_{tag} = g_{tag} g_{reader} P_{reader} \left(\frac{\lambda}{4\pi r}\right)^2 \quad (2.13)$$

where g_{tag} is the tag antenna gain, g_{reader} is the reader antenna gain, P_{reader} is the input accepted power to the reader antenna, λ is the wavelength in free space and r is the distance between the tag and the reader antenna. In order to activate the microchip, a threshold amount of power (P_{th}) is collected by the antenna and transmitted to the chip in order to activate it [25], [4]. The power delivered to the IC chip P_c is given by:

$$P_c = P_{tag} \times \tau \quad (2.14)$$

Where P_{tag} is the power collected by the tag antenna and τ is the power transmission coefficient (PTC). τ is given by:

$$\tau = \frac{4R_c R_a}{|Z_a + Z_c|^2}, \quad 0 \leq \tau \leq 1 \quad (2.15)$$

τ describes matching the antenna and IC chip impedances. Its value has a range from 0 to 1, where $\tau = 0$ means totally mismatching and $\tau = 1$ means ideal matching [34], [25]. Since the microchip

acts as a storage device, it is highly capacitive (X_a is negative). Therefore, to realize an ideal impedance matching $Z_A = Z_c^*$ the antenna impedance Z_A should be inductive (X_a is positive). Besides computing τ , calculating the power reflection coefficient (PRC) and return loss (S_{11}) are effective methods to check the impedance mismatching between the tag antenna and the IC chip. The power reflection coefficient describes the amount of reflected electromagnetic waves due to impedance mismatch over the incident wave. Thus, minimizing PRC as possible is recommended. The return loss RL (S_{11}) is expressed as [41], [42]:

$$S_{11} = \frac{Z_c - Z_a^*}{Z_c + Z_a} \quad (2.16)$$

$$\tau = 1 - |S_{11}|^2 \quad (2.17)$$

Voltage standing wave ratio VSWR is another method to indicate the power delivered by the antenna. VSWR is formed when an amount of the transmitted power is reflected due to impedance mismatch. VSWR is expressed as [43]:

$$\text{VSWR} = \frac{1+|\Gamma|}{1-|\Gamma|} = \frac{1+|S_{11}|}{1-|S_{11}|} \quad (2.18)$$

$$\Gamma = \frac{V_r}{V_i} = \frac{Z_a - Z_c^*}{Z_a + Z_c} \quad (2.19)$$

where Γ is the voltage reflection coefficient at the input terminals of the antenna, V_r and V_i are the amplitude of the reflected wave and the amplitude of the incident wave respectively.

Higher VSWR means higher reflected wave due to impedance mismatching. Thus, for ideal case (perfect impedance matching) $\text{VSWR} = 1$ [43].

2.5.6 Read Range

Read range or detection distance is an important parameter to evaluate antenna performance. Read range is defined as the maximum distance that the tag could be detected from by the reader. In other words, the read range means the maximum distance at which the tag is still able to receive enough power to operate and retransmit the signal to the reader. The maximum achievable read range can be expressed using Friss formula [38]:

$$r_{\max} = (\lambda/4\pi) \sqrt{\frac{P_{\text{EIRP}} \times G_a \times \tau}{P_{\text{th}}}} \quad (2.19)$$

since $G_r = G_a \times \tau$;

$$r = (\lambda/4\pi) \sqrt{\frac{P_{\text{EIRP}} \times G_r}{P_{\text{th}}}} \quad (2.20)$$

where:

λ is the wavelength at the antenna resonance frequency in meters, P_{EIRP} is the regulated equivalent isotropically radiated of the reader (4 W at North America), G_r is the antenna realized gain, P_{th} is the threshold (minimum) power of the selected IC chip and τ is the power transmission coefficient, $\tau = 1$ for perfect matching.

Example 2.1: Suppose UHF RFID tag antenna proposed in [7] operates at 886.5 MHz resonance frequency with a realized gain of -0.53 dBi. The chip sensitivity is -8 dBm and the regulated power of the reader is $P_{\text{EIRP}} = 3.28$ W. Calculate the tag antenna maximum read range.

By using equation (2.20): $\lambda = \frac{c}{f} = \frac{3 \times 10^8}{886.5 \times 10^6} = 0.3384$ m, $G_r = -0.53$ dBi = $10^{\frac{-0.53}{10}} = 0.885$,

$$P_{\text{th}} = -8 \text{ dBm} = 10^{\frac{-8}{10}} = 158.49 \mu \text{ w thus, } r_{\max} = \left(\frac{0.3384}{4\pi} \right) \sqrt{\frac{3.28 \times 0.885}{158.49 \times 10^{-6}}} = 3.7 \text{ m.}$$

2.5.7 Fabrication Material and Process

Tag antennas are made from a thin highly conductive material like copper, silver and aluminum. Silver is the most effective one but, due to its high cost, copper is widely used instead. However, the material of the chosen tag antenna substrate should be low cost, low permittivity and low loss characteristics. The substrate material should provide resistance to various environmental conditions such as heat, vibration, sunlight, moisture and chemicals. Moreover, the substrate material must provide a smooth surface for printing the antenna layout, stability and durability under different operating conditions. The common materials used for the substrate are FR4, PVC, polymers, Polyethylenetherephthalate (PET) and polyesters. The material of the substrate may affect the antenna's operating frequency therefore it should be considered through the antenna tuning [9], [44].

2.5.8 Proximity to Object

RFID system has various applications. Therefore, the tag is attached to different object materials with a different dielectric constant, which affects the tag antenna performance. Whereby, the frequency is detuned and the tag performance is degraded. Thus, the backing object material is considered while tuning the antenna parameters through the design processes [39].

2.6 RFID Applications

RFID systems are used almost in all mainstream fields. It is applied for hundreds, even thousands of various applications. In this section, several RFID applications in different fields are presented.

- **Inventory Management**

Inventory management is one of the important supply chain elements. It has various aspects such as controlling, monitoring, administrating, storing and lastly using the materials for selling a product. The inventory management faces inaccuracy due to a mismatch between the inventory records and the actual amount of available products for sale. RFID technology highly improved inventory system management. Whereby RFID tags can be read through items and many tags can be scanned at one time. The benefits of RFID technology speed up the process of inventory management and reduced error rate thus, provide highly accurate inventory records [45].

- **Baggage Applications**

Package delivery and bagging handling is a complex task and requires a large number of human resources which needs high cost. The employees do several operations from receiving the packages, assembling, sorting and distributing. Human presence causes a high error rate. On the other hand, using the RFID system for packaging and baggage firms including the airline industry reduces the human involvement and the system complexity through automating the whole process which provides high speed, accuracy and reducing cost [1].

- **Toll Road Applications**

RFID provides automatic toll collection and maintains the traffic flow without vehicles stopping for payment. In such an application, vehicles pre-pay their toll monthly or yearly. The RFID reader recognizes and records each vehicle's entry at each toll that is calculated later on by a programmable application. In addition, such application supplies statistical data for the roads which can be used for improvements and analysis.

- **Healthcare application**

In health care systems, there is a need for increasing efficiency, visibility and collecting data of relevant interactions. RFID enhanced the healthcare systems in many ways such as drugs transportation, blood samples administrations, patients' notes management, equipment handling and others. The RFID system provides instantaneous information about the tagged objects or people which provides accurate and up-to-date data of these objects' processes. Thereby time consumption and error rates are reduced [1].

RFID is a wireless communication technology that provides automatic items identification without a line of sight. Tags and readers are the main components of the RFID system. Tags are classified as passive, active or semi-active and readers could be fixed, handheld or mobile. Passive tags are activated by the reader's signals. To receive the maximum amount of power, optimal impedance matching between the tag's antenna and the IC chip should be achieved. Moreover, the radiation pattern, realized gain, read range, tags and objects material all determine the tag's performance. Several impedance matching techniques and the metallic object effect will be explained in the next chapter.

Chapter 3

Passive UHF RFID Tag Antenna

Chapter Three

Passive UHF RFID Tag Antenna

This chapter contains three main parts. Since the impedance matching between the tag antenna and the IC chip is one of the most important passive tag antenna design considerations, basic impedance matching techniques used in UHF RFID tag antenna design are presented in the first part. Then, a brief background of folded dipole antenna is introduced, where it is used in the proposed design. Next, as the presence of metals effect is one of the main challenges in designing tag antennas, the metallic effect and several approaches to overcome its effect are discussed in the second part. Finally, in the third part, the design methodology of passive UHF RFID tag antenna is illustrated.

3.1 Impedance Matching Techniques for UHF Tag Antennas

Several impedance matching techniques which are widely used by RFID tags are presented in this section.

3.1.1 T-Match Method

T-match connection is one of the shunt-matching effective techniques. In order to change the planar dipole with length l input impedance, a short-circuited stub with an additional dipole with length a ($a < l$) is embedded to the large dipole at a distance of $a/2$ from its center. The two dipoles are separated by distance b , and the antenna source (RFID chip) is attached at the center of the small one. The T-matching method configuration and equivalent circuit are illustrated in Figure

3.1. The conjugate impedance matching between the RFID tag antenna and the IC chip could be achieved by tuning a, b and w parameters.

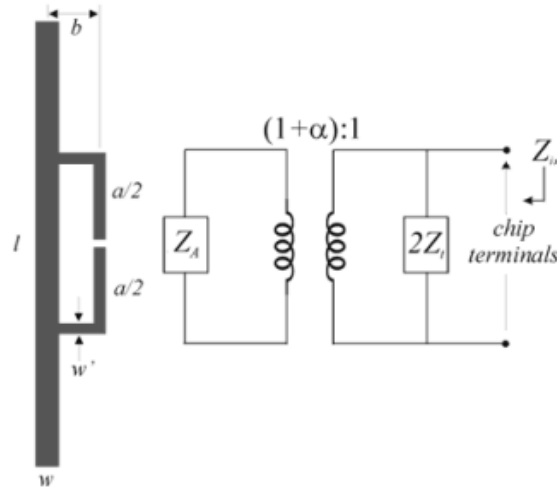


Figure 3.1 The T-match configuration and its equivalent circuit.

In general, the T-match performs as an impedance transformer. It has inductive resulted input impedance for dipoles with $\lambda/2$ length, and it could be inductive and capacitive for small dipoles [46].

3.1.2 Inductively-Coupled Method

In this method, the RFID chip is attached at feed loop terminals, where the feed loop is placed near a long dipole with length l . The communication is formed through mutual coupling between the radiator and the feed loop. According to Figure 3.2:

R_{rb} is the resistance of the radiating body and R_{loop} is the feed loop resistance. Mutual coupling and self-inductance of the feed loop are denoted by M and L_{loop} respectively.

The real part (R_{zin}) and imaginary part (X_{zin}) are given by [46]:

$$R_{zin} = \frac{(2\pi f_0 M)^2}{R_{rb}} + R_{loop} \quad (3.1)$$

$$X_{in} = 2\pi f_0 L_{loop} \quad (3.2)$$

From the equations, it can be noticed that the resistance is controlled by M and R_{loop} and the reactance is affected by L_{loop} .

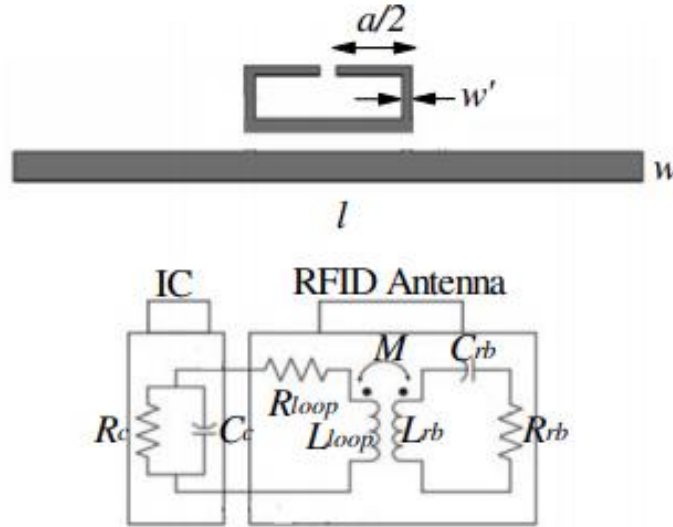


Figure 3.2 Loop inductively-coupled method and its equivalent circuit.

Hence, at the design stages the dimensions of the loop are tuned first to achieve proper conjugate impedance matching with the IC chip. Then adjust the distance between the loop and the dipole to match the chip resistance [46].

U-shaped inductively coupled feed is another inductive coupling approach, which is used in RFID tag antenna design to utilize conjugate impedance matching between the tag antenna and the IC chip [10] and lately, the U-shaped inductive coupling f was used for gain enhancement in [47]. A U-shaped inductively coupled method applied on a coplanar tag antenna which used in [9] is illustrated in Figure 3.3.

The coupling strength is controlled by the U-feeder length and width beside the gap between the feeder and the transmission line.

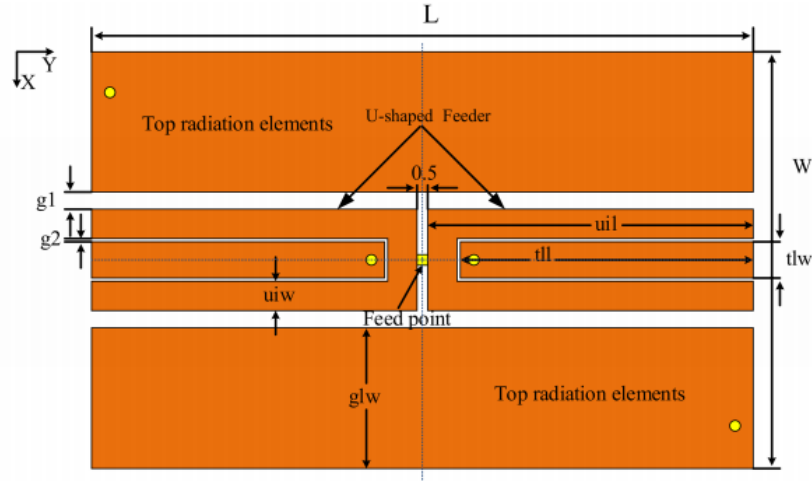


Figure 3.3 A U-shaped inductively coupled feed coplanar tag antenna.

The input impedance of the antenna is expressed as follow:

$$Z_{in} = R_{zin} + jX_{zin} = \frac{(2\pi f_0 M)^2}{Z_{ant}} + Z_{ufeed} \quad (3.3)$$

where Z_{ant} is the radiating body impedance and Z_{ufeed} is the U-shaped feeds impedance which is given by:

$$Z_{ufeed} = 2R_u + 2\pi f_0(2L_u) \quad (3.4)$$

Where R_u and L_u are the U-shaped feed resistance and self-inductance respectively.

3.1.3 Nested-Slot Method

This method is used for suspended patches or large planar dipoles. The nested-slot shown in Figure 3.4 is acting as a tag antenna impedance transformer. Since each tooth of the slot provides radiation and energy storage. Thus, by tuning the slot profile parameters a and b the tag impedance

will be change. On the other hand, adjusting the length of the patch l affects the tag antenna gain [46].

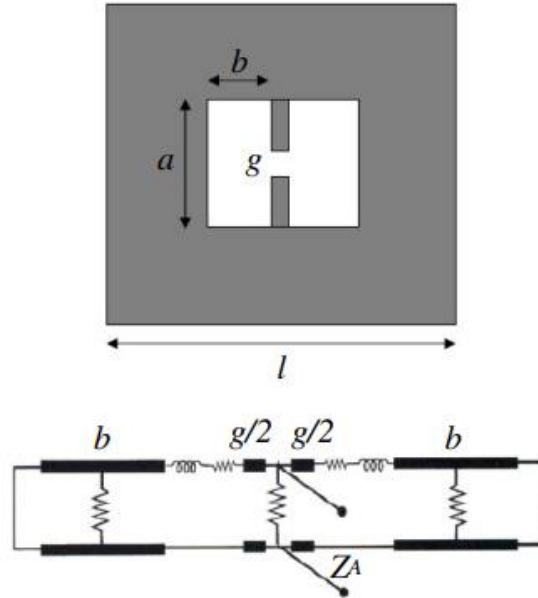


Figure 3.4 The nested-slot configuration and its equivalent circuit.

3.1.4 Open Stubs Method

Loading open stubs to the antenna radiating body is an effective method to reduce the resonance frequency, where the tag resonance frequency can be fine-tuned by changing the open stubs number and their length. Figure 3.5 shows RFID tag antenna design in [5] that is composed of a circular patch that has a nested slot in the middle loaded with four open identical stubs. The short stubs that hold the long open ones are characterized as inductors L_{TS} and the four long open stubs are represented as parallel lumped elements inductor L_{TS} and capacitor C_{TS} .

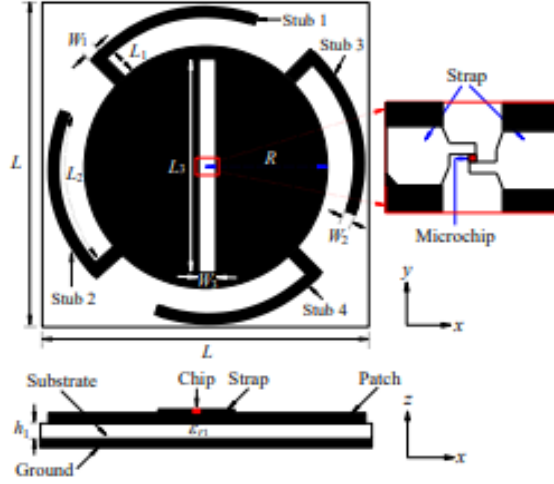


Figure 3.5 A slotted circular patch loaded with open stubs.

Each stub inductance is calculated by [5]:

$$L_{LS} = 2L \left\{ \ln \left[\frac{2L}{W+t} \right] + 0.50049 + \left[\frac{W+t}{3L} \right] \right\} \quad (3.5)$$

where L is the length of the stub, W is the width of the stub and t is the copper layer thickness. The capacitance formed between the ground and the stub is given by:

$$C_{LS} = \frac{\epsilon A_T}{h_1} \quad (3.6)$$

where;

$$\epsilon = \epsilon_0 \epsilon_{r1} \quad (3.7)$$

A_T is the total area of the stub surface, h_1 is the substrate thickness and ϵ_{r1} is the substrate dielectric constant.

Antenna patch and ground are modeled as resistor (R_a), capacitor (C_a) and inductor (L_a) all in parallel are expressed by Z_a . Thus, total input antenna impedance (Z_{antenna}) is given by:

$$Z_{\text{antenna}} = \frac{Z_a(Z_{\text{totalstubs}})}{Z_a + Z_{\text{totalstubs}}} \quad (3.8)$$

where

$$Z_a = \frac{-\omega R_a L_a}{-\omega L_a + j(R_a - \omega^2 R_a L_a C_a)} \quad (3.9)$$

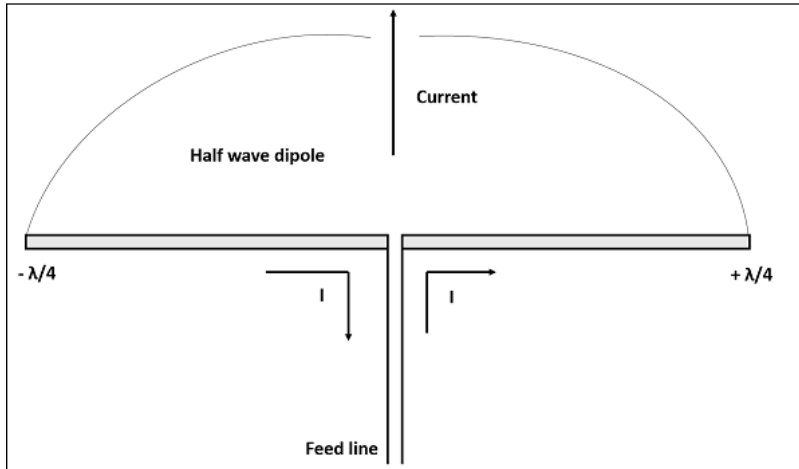
$$Z_{\text{onestub}} = j\omega L_{TS} + \frac{1 + j\omega L_{LS}}{1 - \omega^2 L_{LS} C_{LS}} \quad (3.10)$$

$$Z_{\text{totalstubs}} = Z_{\text{onestub}}/4 \quad (3.11)$$

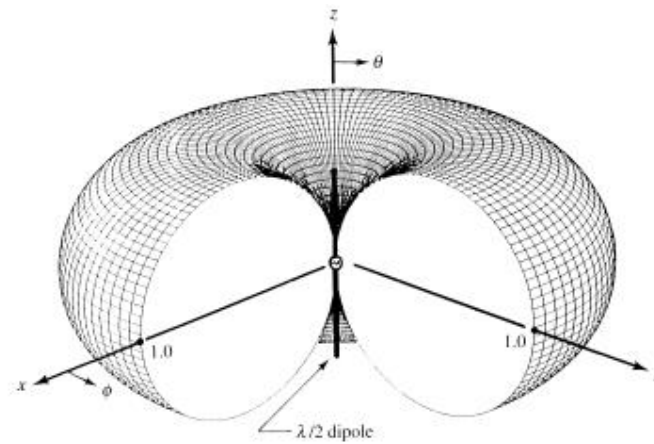
Z_{onestub} is the impedance of a single open stub and $Z_{\text{totalstubs}}$ is the total impedance of the four identical parallel open stubs. The equivalent antenna impedance which could be calculated by the above formulas is compared to the CST simulator resulted one. The calculated and simulated antenna impedances were approximately the same. Thus, the antenna impedance can be simply obtained by simulation.

3.2 Folded Dipole Antenna

Dipole antenna and the dipole variants are the oldest, simplest and least expensive RF (Radio frequency) antennas; therefore dipoles are the most widely used antenna types. A dipole antenna is consisting of two conductive elements split at the center such as metallic wires or rods. Where the length of the metallic wire is approximately equals half of the maximum wavelength in the free space at the operating frequency ($\lambda/2$). The two conductors are fed at the center by a balanced transmission line which carries opposite equal currents on the two conductors [36]. A conventional dipole antenna structure and its radiation pattern are shown in Figure 3.6.



(a)



(b)

Figure 3.6 A half-wavelength dipole (a) structure [48] and (b) radiation pattern [36].

In order to achieve better matching characteristics, a folded dipole antenna is used. A folded dipole is one of the single dipole variants that consists of a basic dipole with an added conductor that connects the dipole ends together (array of two parallel dipoles) forming a rectangular thin loop ($s \ll \lambda$) as shown in Figure 3.7. The folded dipole is operated at a half wavelength of the operating frequency similar to a basic dipole and has the same omnidirectional radiation pattern. A folded dipole with two arms impedance is four times greater than that of an ordinary dipole antenna at

the resonance frequency. Folded dipole is fed by a high characteristic impedance feeder of about 300Ω twin-lead transmission lines. The impedance matching could be fine-tuned by varying the parameters of the dipole arms. Besides, the antenna input impedance is modified by adding multiple folded arms. Moreover, folded dipoles have been examined for UHF tag antenna miniaturizing. Since folding a dipole usually reduces its footprint [36].

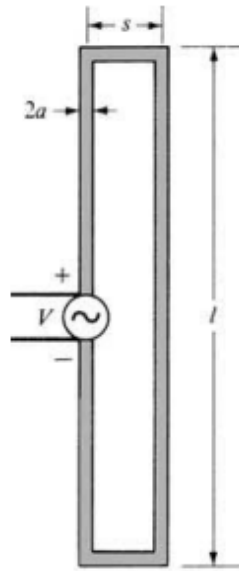


Figure 3.7 A folded dipole structure.

Obtaining a compact RFID dipole tag antenna with a maximum space of 2500 mm^2 operates at the UHF band is unattainable. Since the low profile tag has a very high resonance frequency [38]. Therefore, several techniques are presented in order to reduce and tune the resonance frequency while maintaining the tag size compacted such as loading triangular stubs [11], connecting identical stubs to a circular slotted patch [5], etching a T-matching network and meandered strips [49], embedded of extra arms and outer strip lines at C-shaped resonators [7], adding shorting stubs and notches [50], using U-shaped inductively coupled feed [10], [8] and another various techniques.

3.3 Effect of Metal on UHF RFID Tag

Passive UHF RFID tag antennas have the advantage of low cost and providing a high read range compared to LF and HF tags. However, UHF RFID passive tags suffer performance degradation when they are placed on a metallic object. Where passive tags obtain their power energy from the reader's electromagnetic waves, then the obtained energy is converted to electrical energy which powers up the IC chip. If the interrogation field from the reader antenna reaches the tag is insufficient, the RFID tag will be unreadable. That happens when the RFID tag is placed on a metallic object. To understand the electromagnetic waves behavior near a metallic surface, Maxwell's electromagnetic boundary conditions theory is presented.

Consider two mediums in space where medium one characterized by magnetic permeability μ_1 , dielectric permittivity ϵ_1 and electric conductivity σ_1 , and medium 2 with μ_2 , ϵ_2 and σ_2 , the boundary between medium 1 and 2 is expressed by the electromagnetic boundary conditions as follow:

$$\hat{\mathbf{n}} \times (\mathbf{E}_2 - \mathbf{E}_1) = \mathbf{0} \quad (3.12)$$

$$\hat{\mathbf{n}} \cdot (\mathcal{D}_2 - \mathcal{D}_1) = \rho_s \quad (3.13)$$

$$\hat{\mathbf{n}} \times (\mathcal{H}_2 - \mathcal{H}_1) = \mathcal{J}_s \quad (3.14)$$

$$\hat{\mathbf{n}} \cdot (\mathcal{B}_2 - \mathcal{B}_1) = 0 \quad (3.15)$$

where $\hat{\mathbf{n}}$ is the unit normal vector to the boundary, \mathbf{E} and \mathcal{D} are the electric field intensity and flux density respectively, \mathcal{H} and \mathcal{B} are the magnetic field intensity and flux density respectively, ρ_s is the surface charge density and \mathcal{J}_s is the surface current density. Suppose medium one is a perfect electric conductor (PEC), thus medium one has an infinite conductivity ($\sigma_1 \rightarrow \infty$).

So, the electric field is zero in this medium ($\mathbf{E}_1 = \mathbf{0}$). Subsequently, $\mathcal{D}_1 = 0$, $\mathcal{H}_1 = 0$ and $\mathcal{B}_1 = 0$.

The boundary conditions become as follow:

$$\hat{\mathbf{n}} \times (\mathbf{E}_2) = \mathbf{0} \quad (3.16)$$

$$\hat{\mathbf{n}} \cdot (\mathcal{D}_2) = \rho_s \quad (3.17)$$

$$\hat{\mathbf{n}} \times (\mathcal{H}_2) = \mathbf{J}_s \quad (3.18)$$

$$\hat{\mathbf{n}} \cdot (\mathcal{B}_2) = \mathbf{0} \quad (3.19)$$

from the above equations, it is observed that not all the magnetic field components are present near a PEC surface. Since $\hat{\mathbf{n}}$ is the unit normal vector to the boundary, the dot product (.) results in a normal component and the cross product (\times) results in a tangential component. Hence, the magnetic field has only tangential components next to the PEC medium, and has no normal (perpendicular) components directly to the PEC surface. While the electric field has only normal components to the PEC surface and has no tangential components directly next to the PEC, any RFID tag depends on either the magnetic field normal component or the electric field tangential component to operate faces performance degradation when placed on a metallic object. Figure 3.8 (a) and (b) illustrate electric and magnetic fields near a metallic surface. Besides, when uniform electromagnetic wave incidences to a boundary of a PEC medium, the incident wave is reflected with phase reversal. Subsequently, the reflected electric field cancels out the incident one, therefore the electric field will zero at the boundary. On the other hand, the incident magnetic field is doubled at the boundary [35], [51].

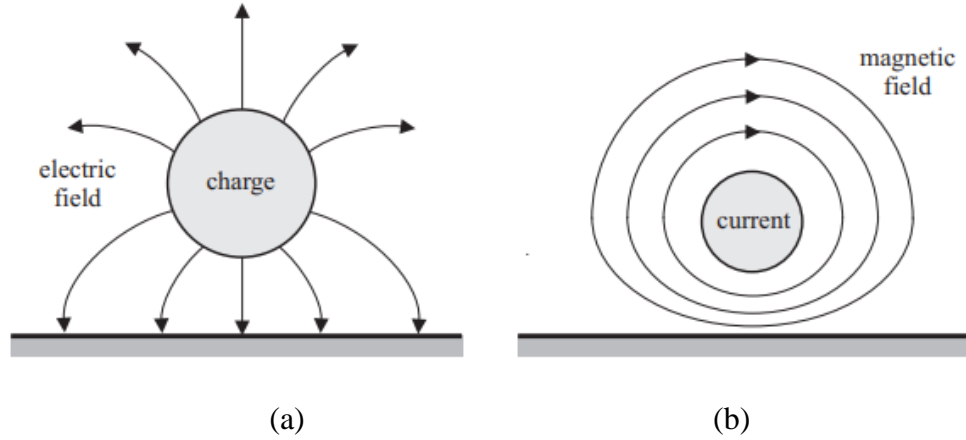


Figure 3.8 Simple illustration of the boundary conditions where (a) electric fields and (b) magnetic fields near a metallic surface.

The metallic surface affects the RFID tag antenna parameters, where the presence of metal causes changes in antenna impedance, radiation pattern, directivity, bandwidth and efficiency. The change in the RFID tag antenna impedance causes two main issues. The first one is the impedance mismatch between the tag antenna and the IC chip. Since the effective impedance matching between the tag antenna and the chip provides the maximum power transfer, the impedance mismatch reversely affects the amount of the transferred power from the tag antenna to the IC chip which also affects the read range. The second issue is the effect on the resonance frequency of the RFID tag. The resonance frequency f_r for a tuned circuit is given by [52]:

$$f_r = \frac{1}{2\pi\sqrt{LC}} \quad (3.20)$$

Where L is the inductance and C is the capacitance of the circuit. Hence, the change in the tag antenna reactive impedance part due to a metallic surface directly affects the resonance frequency, which causes detuning and degradation in the read range. The degradation of the read range depends on the resonance frequency deviation amount [52].

After the discussion of the metallic surface effect on the RFID tag antenna performance, some solutions will be presented in the next section.

3.4 Passive UHF RFID Tag Antennas for Metallic Objects

In order to solve the metallic effect issues, different approaches have been proposed by the researchers as follow:

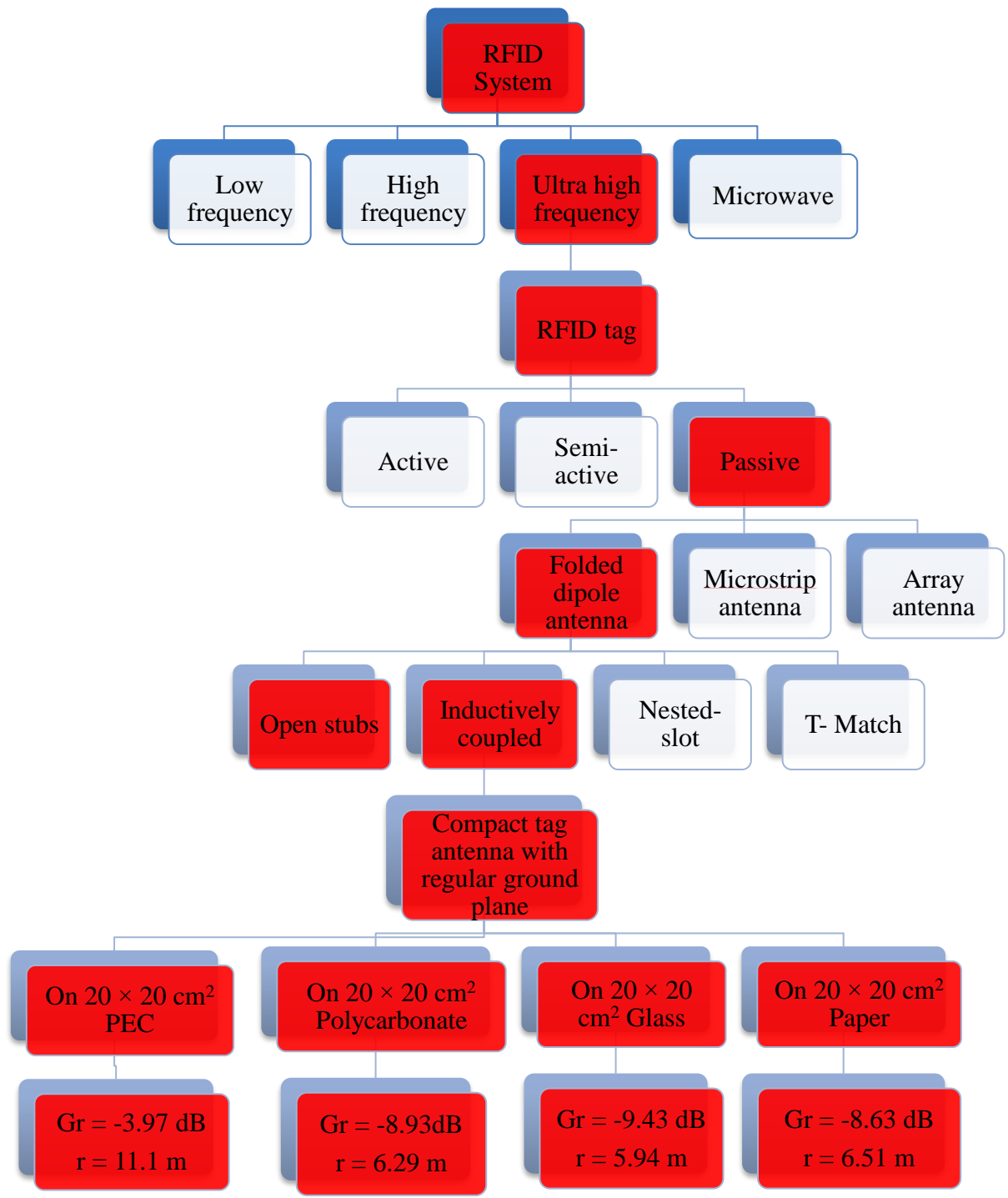
- Using an artificial magnetic conductor (AMC) structure is one of these approaches, whereby the AMC structure reflects the incident wave in-phase at the tag surface while the AMC ground plane is placed behind the tag at a particular distance [53].
- Using an Electromagnetic Bandgap (EBG) is another method. EBG is called photonic band gap, is a kind of material that could be used as a ground plane of dipole tag antenna due to its unique property of selective suppression of the incident electromagnetic wave. Thence, EBG is used to overcome the impedance mismatch issue due to the back metal plate effect at a certain frequency band (RFID band). Moreover, EBG ground plane is used to enhance the tag antenna gain [53], [12].
- Using foam [6] or an air gap [11] to separate the tag antenna from the back metallic object is another method.
- The utilization of a planar inverted-F antenna (PIFA) [54] and foam-attached tag [50].
- Using low loss tangent thick substrate [55], utilization of parasitic elements [56], using two substrates [9] and much more.

Although these approaches showed an improvement of the tag antenna performance near metallic objects, the fabrication cost and complexity were significantly increased due to costly substrate, using metallic via, shorting stubs, shorting walls and high thickness structure.

In this project, the tag antenna is composed of a single layer implemented on a cheap dielectric polytetrafluoroethylene (PTFE) substrate. The tag antenna is specially designed to work effectively on metallic objects without the requirement of any shorting elements or complicated fabrication works. Thus, the substrate is coated with copper as a ground plane and placed directly on a metallic plate through the design process. The properties of metal are used for enhancing the read range if the correct tag antenna design is implemented.

3.5 Scope of Research

After the discussion of the RFID system and studying the RFID tag antenna design considerations besides the review of various impedance matching techniques, the following flow chart illustrates the scope of this research. A passive UHF RFID tag antenna is designed. The folded dipole antenna type is used to design the antenna configuration with a regular ground plane. Both adding open stubs and inductive coupling are used to realize the impedance matching between the tag antenna and the IC chip. Thereafter, the tag is placed on different metallic and dielectric plates whereby the realized gain and read range of the tag was investigated. The methodology of the design is presented in the next section.



3.6 Design Methodology

Figure 3.9 summarizes the methodology of designing a passive UHF RFID tag antenna. After determining a certain application, the designer should study the tag antenna design requirements which were presented in section (2.5). Based on the tagged object material and size, frequency regulations and the required read range the design is implemented. Before any fabrication process, the design is implemented and simulated by a 3D full-wave simulator like CST Microwave Studio. Choosing materials of the substrate and antenna is directly determining the tag cost and size as well as the antenna geometry. Varying the antenna dimensions is applied until the design requirements are met. Then, the design is fabricated and tested to make sure that all the application requirements are achieved and finally, it is ready for mass production [39].

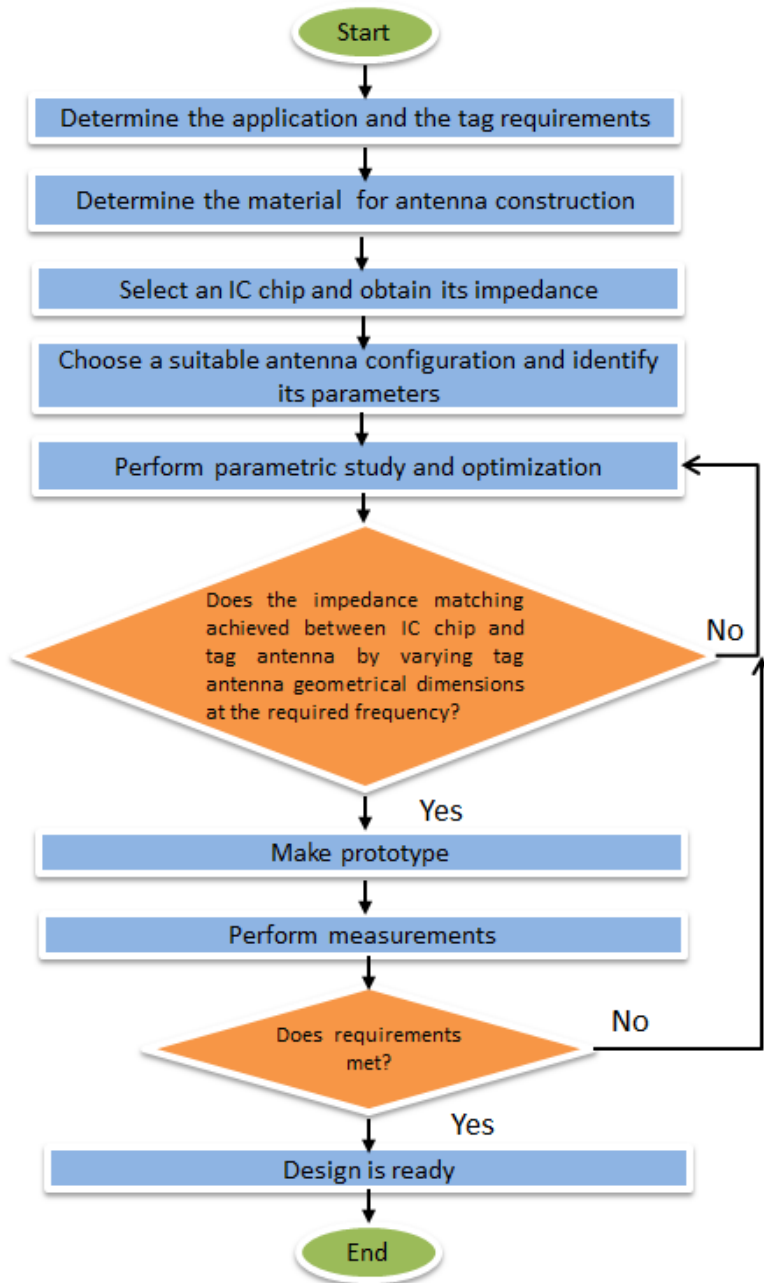


Figure 3.9 Methodology design flow of RFID tag antennas.

Folded dipole antennas are used widely in RFID tags due to their simplicity, small size and low cost. Many impedance matching techniques are used such as T-matching network, inductive coupling and nested slots. However, metallic objects cause impedance mismatching and affect the

tag resonance frequency. Therefore, several solutions are introduced by the researches. In general, to design a tag antenna with a significant performance the metallic object should be considered through the designing process. The proposed design requirements, specifications, design stages and parametric study all are presented in the next chapter.

Chapter 4

A Novel Mutually Coupled Folded Dipole UHF RFID Tag Antenna

Chapter Four

A Novel Mutually Coupled Folded Dipole UHF RFID Tag Antenna

In this chapter, a novel miniature UHF tag antenna for metallic objects is designed. First, the design and simulation process using the CST Microwave Studio software is presented. Then, the tag antenna structure is presented. Finally, the main design parameters varying effect is analyzed and investigated.

4.1 Design and Simulation Process

According to Figure 3.9, the first process of designing the tag antenna is determining the application and tag requirements. The proposed design should work effectively for metallic object applications. Moreover, the main requirement of the tag is to minimize the size and cost as possible. The selected materials and IC chip are the same as those used in [8]. The materials of the antenna configuration and the substrate are copper and polytetrafluoroethylene (PTFE) respectively. Higgs 4 chip is used which has an input impedance of $20.97 - j193.16 \Omega$ at 915 MHz and a reading sensitivity of -20.5 dBm. The chip has two copper straps with dimensions illustrated in its datasheet [57] which were precisely modeled by the simulation. The design is implemented and simulated by CST Microwave Studio software. The proposed tag antenna is placed on a 20×20 cm² perfect electric conductor PEC plate with 1 mm thickness during the entire simulation process.

4.1.1 Simulation Using CST Software

The simulation work is important to predict the tag characteristics before any fabrication process. Computer simulation technology CST microwave studio is a powerful tool for electromagnetic design and analysis. There are several computational electromagnetic methods. The computational

electromagnetic methods differ based on the application domain. Thus, the CST software contains four solvers (Frequency-domain solver, transient solver, eigenmode solver and integral equation solvers). Each solver uses a different computational method to best fit the application field. The study of electromagnetic computational methods is not within the scope of this thesis. Further details of several methods of electromagnetic computing are found in [58]. Moreover, solvers' features and their applications are explained in the CST user guide [59]. However, The CST recommends the appropriate solver based on the selected application field by the user.

To create the project template, first, the CST program asks you to select the application area and the workflow. Next, the program asks you to select the antenna type and recommends solvers based on the selected workflow. Then, select the units of the dimensions, frequency, capacitance and other parameters shown in the template. Finally, define the simulation settings by determining the range of frequency, select the field monitors and define the frequency value of the monitor. Now, the template is ready.

For this research work, Microwave & RF application area and antennas workflow are chosen. The selected antenna type is RFID. The selected solver is the frequency domain solver which is used for the RFID application field (it is recommended by the CST already). The unit of dimensions is set to (mm) since the geometry of the RFID tag is compact. The frequency unit is set to (GHz). Finally, the far-field monitor is selected to monitor the antenna performance at each frequency in the range of the RFID UHF band (860- 960) MHz.

To implement the design configuration, first, insert the expression and value of each parameter in the specified table. Then, choose a suitable block shape and determine the block material. After that, draw each element of the design by inserting the element dimensions as an expression based on the predefined parameters due to x,y and z coordinates. The design method is explained by an

example in Appendix A. At the end of the design implementation, an excitation is assigned to the simulation structure. The excitation acts as a source to the tag as it is attached across the feed terminal of the antenna structure. In the case of the RFID tag antenna, the IC chip is the excitation element. A discrete port with an impedance of 50Ω is assigned between the antenna feeding terminals (the chip position). Then, an external port with conjugate impedance is attached. The external port impedance is set to the impedance of the selected chip. Finally, the discrete port impedance is normalized automatically to become that for the selected chip [5]. For the Higgs 4 chip, the discrete port impedance is 20.97Ω and the lumped element port (conjugate port) impedance is 0.9005 PF both are defined at terminals of the chip straps terminals.

Finally, run the simulation and investigate the resulted S_{11} , antenna impedance, antenna gain, realized gain and radiation pattern. All details of The CST software features and solvers are available in a full CST user guide in [59]. Full design and simulation tutorials are included.

4.1.2 Higgs 4 chip

The RFID chip is selected according to the determined application. Each chip has specific features. The Higgs 4 is a programmable chip that operates at very low power levels which provides a high read range. The Higgs 4 chip has several applications such as supply chain management, baggage handling and tracking and asset inventory and tracking. The IC chip is represented by its impedance through the simulation as explained in the previous section. More details of the Higgs 4 chip features and applications are found in [60].

4.1.3 Initial Antenna Structure

The total thickness of the tag antenna proposed by [8] was 1.5 mm. The thickness of the copper layer is 0.035 mm and the Higgs 4 chip is used. The antenna configuration is designed at the center of a low-cost dielectric polytetrafluoroethylene (PTFE) substrate with a permittivity of 2.55 (loss

tangent 0.0015). A distance $E= 2$ mm is determined between the antenna and the substrate edges. The width of the U- shaped structure (W) is 2 mm, the separation between the U-shaped feeder and the transmission line (S) is 1 mm. The separation between the U- shaped feeder and the antenna patch S_1 is 0.2 mm.

The mentioned parameters used in [8] are used to design the initial antenna structure of this work. The bottom surface is coated with a thin ground copper layer. The proposed tag antenna is designed to operate at the North America band (902-928MHz). The geometry of the initial folded dipole tag antenna structure is presented in Figure 4.1. Table 4.1 shows the parameters of the initial tag antenna structure. The total size of the design is $30.6 \times 41 \times 1.5$ mm³. The proposed RFID tag antenna is composed of two opposite horizontal outer strips each loaded with five identical vertical open stubs and one shorter and wider open stub in the middle. The identical open stubs connected to the upper and lower strips conversely toward the center forming two symmetric nested combs. The two nested combs are connected at the center by the RFID chip which is attached to the two middle wide open stubs forming the feeding line. The feeding line used in [6] is used in this proposed design with the same length ($L= 15$). The two middle short open stubs width ($W_1= 4$) and the gap between them ($G= 3$) were specifically selected to fit the IC chip straps dimensions. The horizontal gap between the nested combs (A) is laid to prevent overlapping. The dipole antenna structure forms the input impedance network, whereby tuning its dimensions is utilized to achieve the optimal conjugate impedance matching with the IC chip.

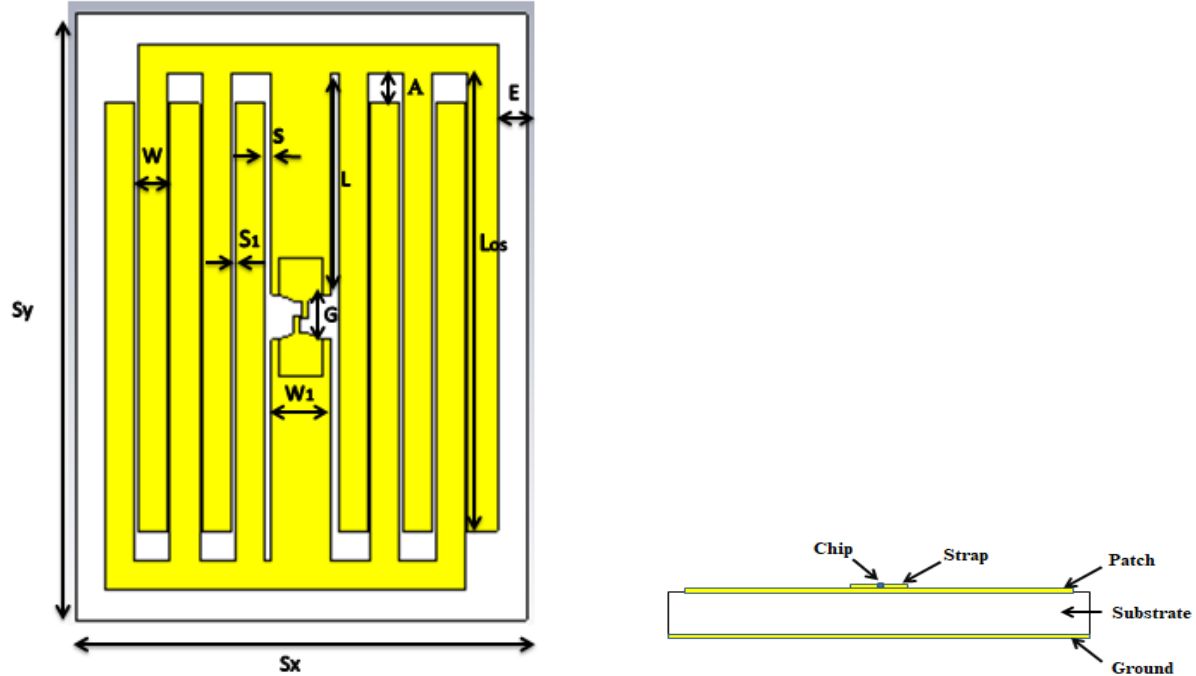


Figure 4.1 Configuration of the initial proposed tag antenna.

Table 4.1 Dimensions of the initial proposed RFID tag antenna (mm).

Parameter	L	W	W ₁	G	A	S	S ₁	E	S _x	S _y
Value (mm)	15	2	4	3	2	0.5	0.2	2	30.6	41

According to Figure 4.1, the substrate dimension S_x and S_y besides the open stub length L_{os} are expressed as: ($S_x = W_1 + 2 \times S + 8 \times S_1 + 10 \times W + 2 \times E$), ($S_y = 2 \times L + G + 2 \times W + 2 \times E$) and ($L_{os} = 2 \times L + G - A$).

Each open stub acts as an inductor thus; using the open stubs is useful for tuning the resonance frequency [5].

After determining the initial value of each parameter, the parameters are tuned to realize the conjugate impedance matching between the antenna and the IC chip. Varying the tag antenna parameters is applied until the reflection coefficient S_{11} value becomes lower than -10 dB at the required band (902- 928 MHz). S_{11} indicates the power reflected due to the impedance

mismatching between the tag and the IC chip. Thus, minimizing the S_{11} value as possible is essential where this means that most of the wave is transmitted. Back to equation (3.5), adjusting the length of the open stubs (L_{os}) tunes the open stubs inductance which controls the resonance frequency and the antenna reactance. According to the above expression of L_{os} , the length of the open stubs depends on the feeding line length (L) and the separation between the two symmetric combs (A). The reflection coefficient S_{11} response of the initial design with different values of (L) is shown in Figure 4.2. The antenna has no response at the required frequency band (902- 928) MHz. The S_{11} is > -10 dB meaning that most of the wave is reflected due to the impedance mismatching between the tag antenna and the IC chip. The S_{11} is high even when the length of the open stubs is increased.

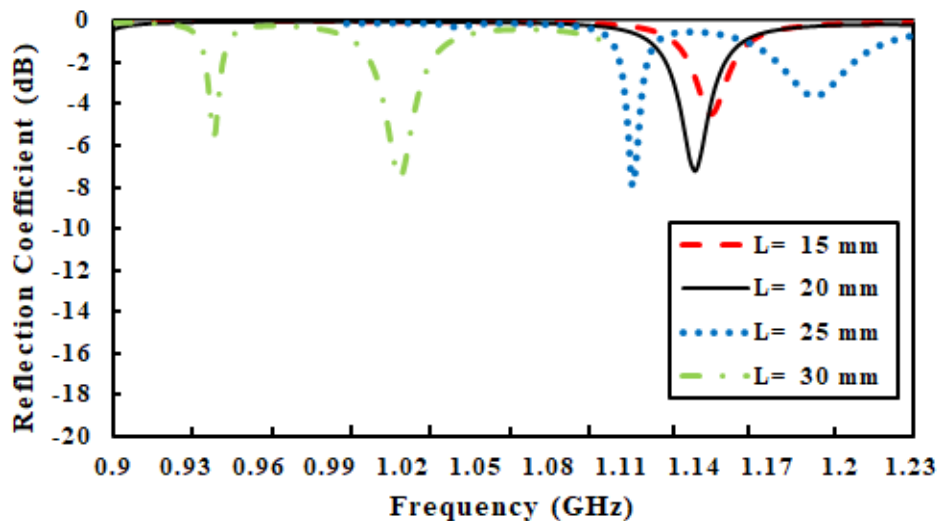


Figure 4.2 Simulated reflection coefficient response of the initial antenna structure at different L values.

Many trials of tuning the antenna parameters were applied. However, the antenna still has a high S_{11} ($S_{11} > -10$ dB) in the required band meaning that the antenna and IC chip impedances are mismatched. The initial proposed tag has no response at the required frequency.

To increase the antenna inductance, two additional open stubs are added at the lower and upper sides with the same parameters. The additional open stubs are attached in a way such that the antenna structure remains symmetric. The total size of the tag is $39.4 \times 41 \times 1.5 \text{ mm}^3$. The reflection coefficient S_{11} response of the tag antenna with the additional open stubs is shown in Figure 4.3. The result shows that the S_{11} decreased to -22 dB at a resonance frequency of 760 MHz. Loading the additional open stubs increased the tag antenna inductance which shifted down the resonance frequency and realizes conjugate impedance matching between the tag antenna and the IC chip ($S_{11} < -10 \text{ dB}$). However, the resonance frequency is lower than the desired band. Furthermore, different trials were applied by tuning the antenna parameters until the best antenna response is achieved as shown in Figure 4.3.

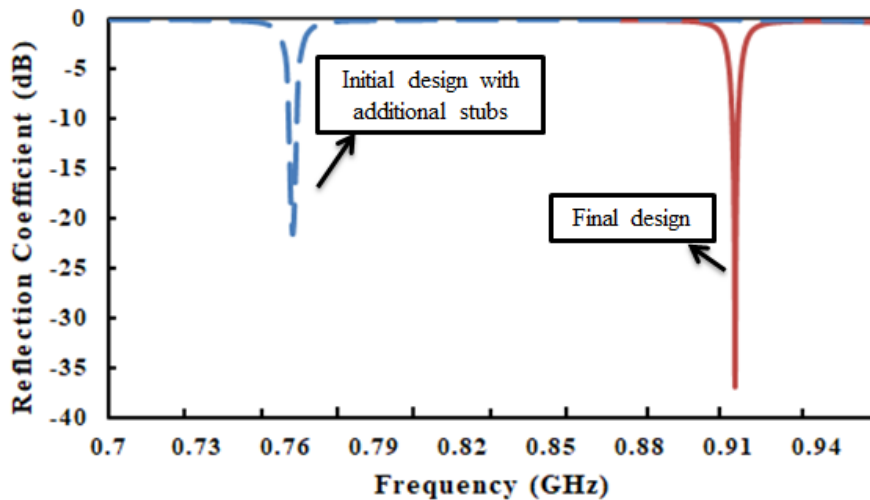


Figure 4.3 Simulated reflection coefficient response of the initial antenna structure with additional open stubs and the simulated reflection coefficient of the final structure.

By readjusting the tag antenna parameters, the S_{11} decreased to -39.5 dB and the resonance frequency increased to 912 MHz. Meaning that an optimal impedance matching between the tag and the IC chip is realized at the required frequency. The final antenna structure and parameters

are illustrated in the next section. In addition, the parametric study and the effect of the open stubs are presented later in this chapter.

4.2 Final Antenna Structure

The geometry of the proposed folded dipole tag antenna is presented in Figure 4.4. The tag antenna design is implemented on a low-cost dielectric polytetrafluoroethylene (PTFE) 55.80×44 mm² substrate with a thickness of 1.43 mm and a permittivity of 2.55 (loss tangent 0.0015). Higgs 4 chip with an input impedance of $20.97 - j193.16 \Omega$ is used. The proposed RFID tag antenna is composed of two opposite horizontal outer strips each loaded with seven identical vertical open stubs and one shorter and wider open stub in the middle. The two nested combs are connected at the center by the RFID chip.

The length of the open stubs depends on the feeding line length (L) and the gap between the two symmetric combs (A). Table 4.2 shows the parameters of the final proposed tag antenna.

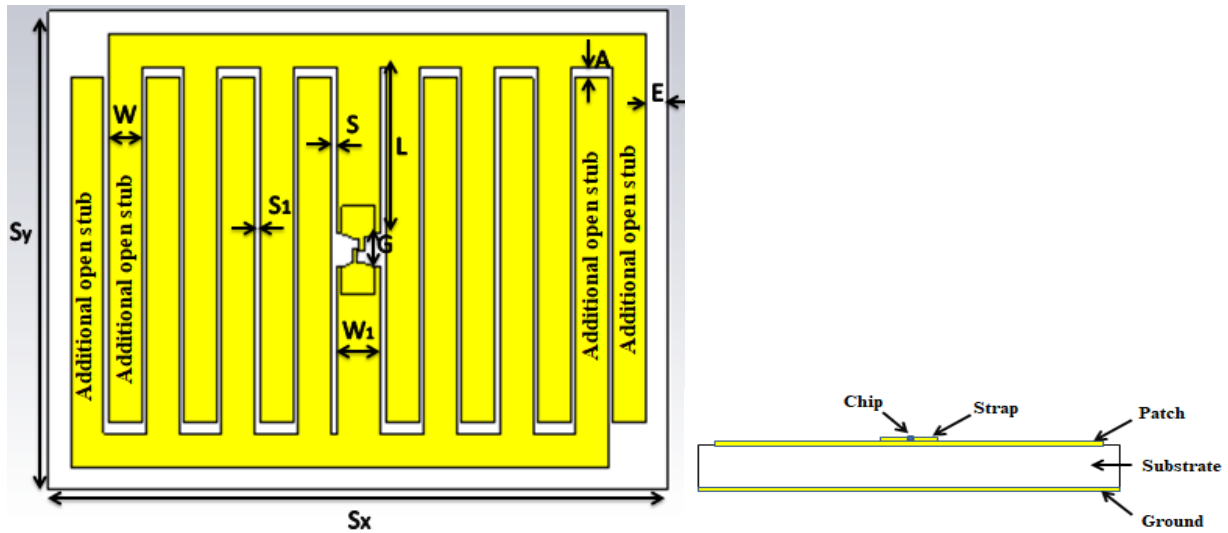


Figure 4.4 Configuration of the proposed tag antenna. ($S_x = W_1 + 2 \times S + 12 \times S_1 + 14 \times W + 2 \times E$).

Table 4.1 Dimensions of the proposed (Final structure) RFID tag antenna (mm).

Parameter	L	W	W ₁	G	A	S	S ₁	S _x	S _y
Value (mm)	15.5	3	4	3	2.1	0.2	0.45	55.8	44

Adjusting (L) and (W) is directly related to the open stubs inductance which affects the reactance of the tag antenna and the resonance frequency, thus both (L) and (W) are tuned accurately to shift down the resonance frequency and minimize the reflection coefficient S_{11} less than -10 dB at the desired resonance frequency. The vertical gap between the nested open stubs (A) affects the length of the open stubs ($L_{os} = 2 \times L + G - A$) and the mutual coupling strength as well as the horizontal gaps between the identical open stubs (S_1) which also controls the coupling strength. Both (A) and (S_1) were tuned precisely to realize the optimal S_{11} value. The effect of the open stubs and the geometrical parameters of the proposed design are presented next.

4.3 The Open Stubs Effect

The effect of the open stubs number is investigated through three stages as follow:

- At the first stage, three open stubs only are added at both upper and lower sides conversely toward the center forming two nested combs each having three identical open stubs and one middle shorter and wider one. The chip is attached in the center at the gap ($G= 3$) between the two middle wide open stubs. The resonance frequency is 2.38 GHz as shown in Figure 4.5 (a). It is too high for RFID implantations.
- At the second stage, two additional open stubs are added at each upper and lower outer strips forming two nested combs each have five identical open stubs. The resonance frequency decreased to 1.69 GHz as shown in Figure 4.5 (a) that is due to the increment in antenna inductance caused by adding the additional open stubs which decreased the resonance frequency. Since open stubs act as inductors, they concentrate the surface current

in the antenna structure which enhances its inductance [5], [7]. Although that, the resonance frequency is still higher than the RFID band.

- Finally, two more additional open stubs are added at each upper and lower side in order to increase the folded dipole antenna inductance which shifted down the resonance frequency to 912 MHz. This is shown in Figure 4.5 (b); it is observed that the antenna impedance matches the IC chip impedance at the proposed RFID frequency band (902-928 MHz).

Adding the additional open stubs at each stage necessarily forms additional U-shaped mutual coupling segments which increase the surface current density and contribute to realize an ideal reflection coefficient [9], whereby U-shaped inductively coupled feed enhances the antenna gain [47].

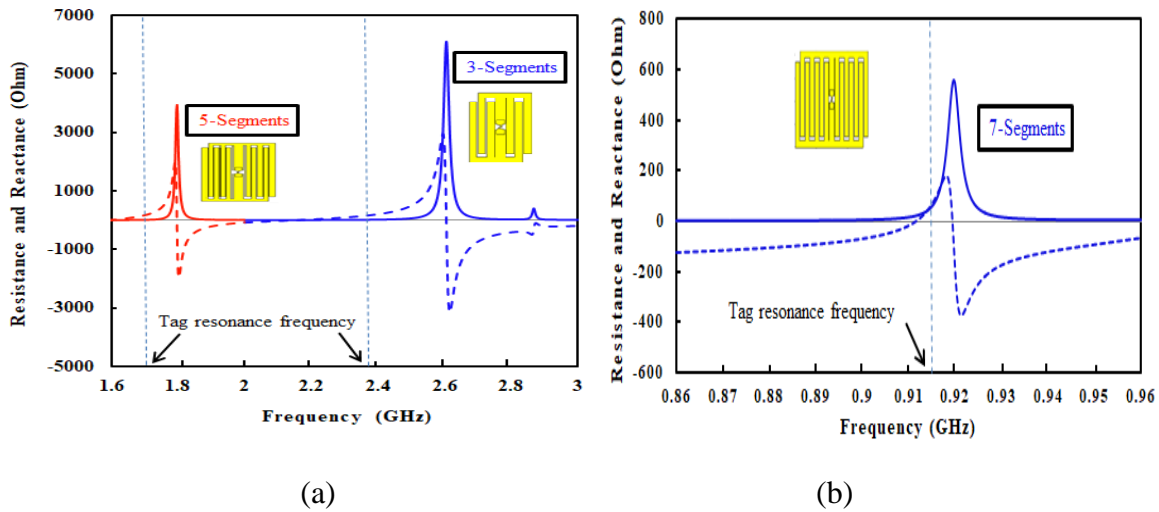


Figure 4.5 Input impedance of the tag antenna at (a) first stage with three segments, second stage with five segments and (b) final stage with seven segments.

Figure 4.6 illustrates the surface current at each stage at their resonance frequencies. It is observed that the surface current increased from 377 A/m to 1212 A/m when the U-shaped segments were

increased from three to five segments. Then, the surface current increased to 2264A/m at the third stage that is composed of seven U-shaped mutual coupling segments.

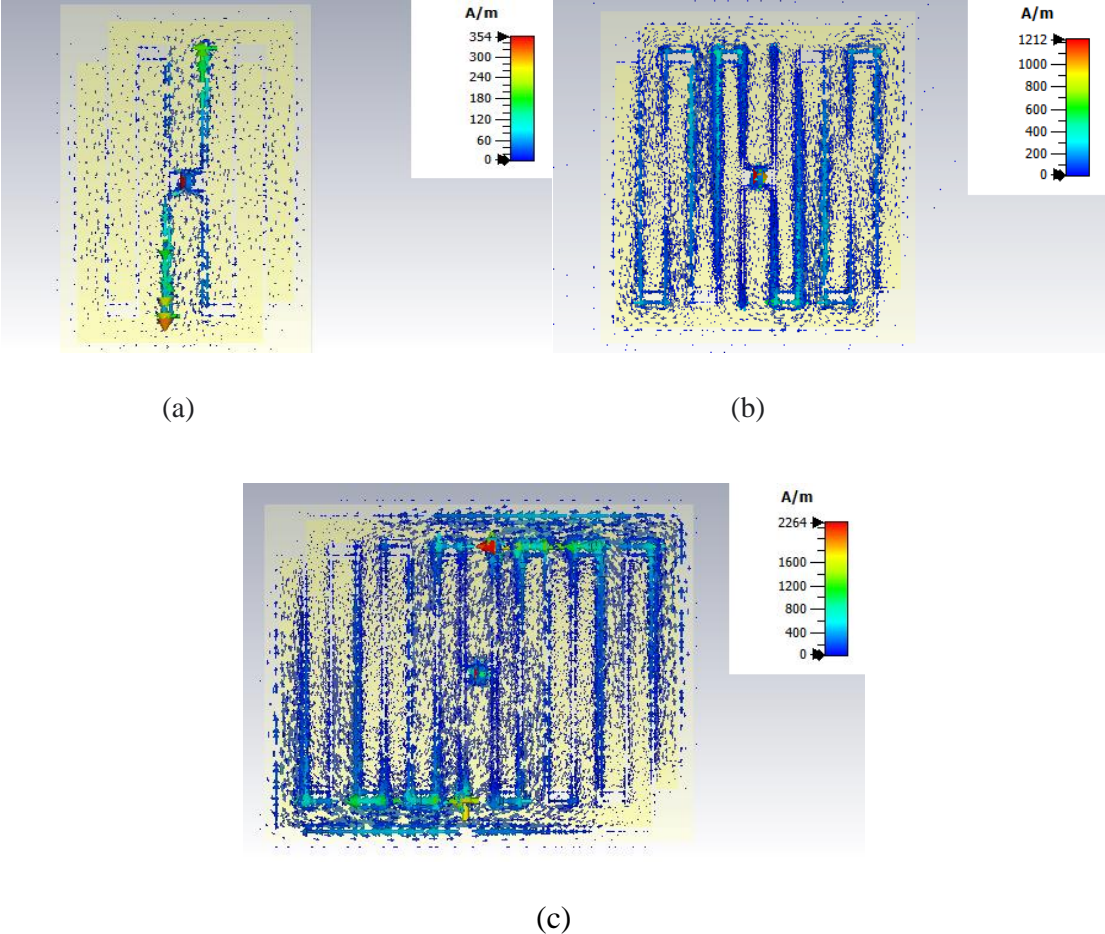


Figure 4.6 Tag antenna’s surface current distribution at the resonance frequency for each design stage; (a) first stage, (b) second stage and (c) final stage.

The additional open stubs and the formed U- shaped segments increased the inductance and the mutual coupling effect. Therefore, increasing the open stubs number increased the surface current which provides a stronger radiation field. Stronger radiation field enhances the antenna which increases the read range.

4.4 Parametric Study

When designing a tag antenna, it is necessary to study the effect of the design important parameters on the tag performance. The feeding line length (L) is directly related to the identical open stubs length ($L_{os} = 2 \times L + G - A$) which provides a flexible tuning mechanism. Thus feeding line length (L) is the main factor in reducing the resonance frequency. The tag performance is investigated according to the reflection coefficient S_{11} response. The simulation results of tuning (L) are shown in Figure 4.7, while (L) is increased from 12.5 mm to 15.5 mm the resonance frequency shifted down from 1.06 GHz to 912 MHz at a rate of 39 MHz/mm. By increasing the length of the open stubs the inductance is increased according to equation (3.5), thus the resonance frequency increased. Back to equation (3.5), the width of the open stub (W) is related to the stubs inductance too, whereby each (L) value has its associated value of (W) to attempt a lower S_{11} value (optimal impedance matching). The effect of varying (W) is shown in Figure 4.8, it can be noticed that the resonance frequency is changed from 984 MHz to 912 MHz at a rate of 72 MHz/mm by varying (W) from 2 mm to 3.5 mm.

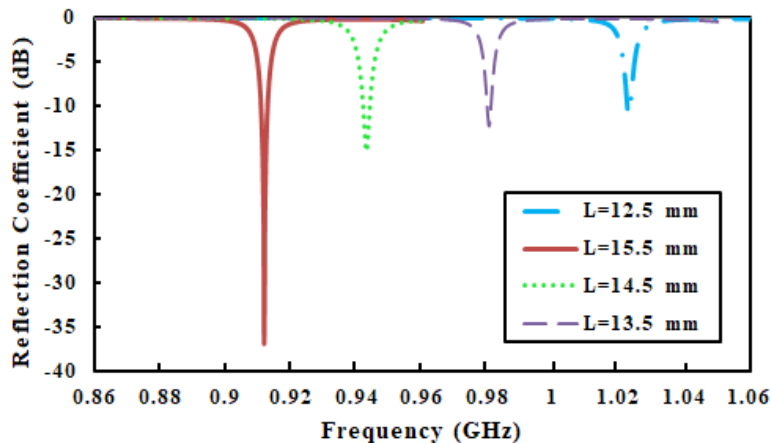


Figure 4.7 Simulated reflection coefficient response at different L values.

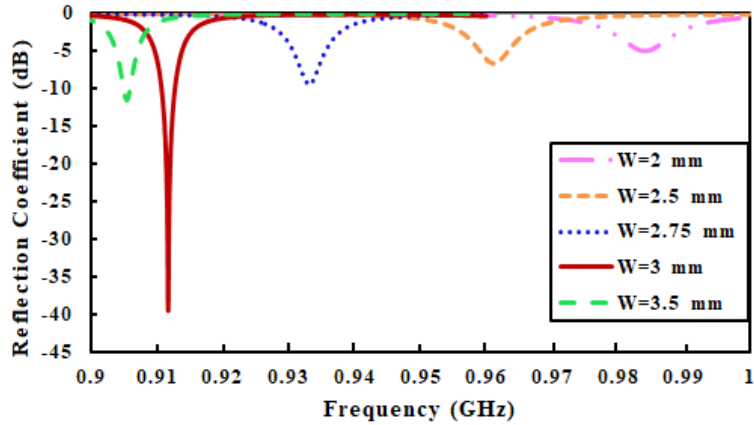


Figure 4.8 Simulated reflection coefficient response at different W_1 values.

Next, (A) effect is studied. Tuning the separations of the U-shaped segment separation of the transmission line controls the strength of the mutual coupling [9]. (A) controls the mutual coupling strength besides its effect on the identical open stubs length ($L_{os} = 2 \times L + G - A$). The simulation effect of varying A is shown in Figure 4.9. The significant tuning of (A) affects the resonance frequency and S_{11} value. The increment of (A) decreases the mutual coupling strength which shifted up the resonance frequency. Thus, (A) is varied by a tiny increment of 0.1 mm at each trial to reach the optimal S_{11} value (-39.56 dB) at the desired resonance frequency. The frequency increased from 911.5 MHz to 912 MHz due to the tiny increment in A from 2 mm to 2.1 mm and the S_{11} value decreased by 5.56 dB.

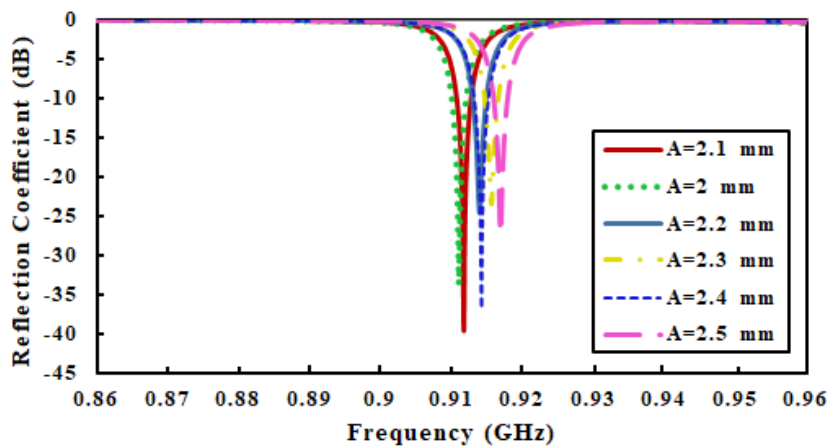


Figure 4.9 Simulated reflection coefficient response at different A values.

Finally, the results of varying S and S₁ are shown in Figure 4.10 and Figure 4.11 respectively. It is observed that by tuning S and S₁ the S₁₁ decreased to -39.56 dB.

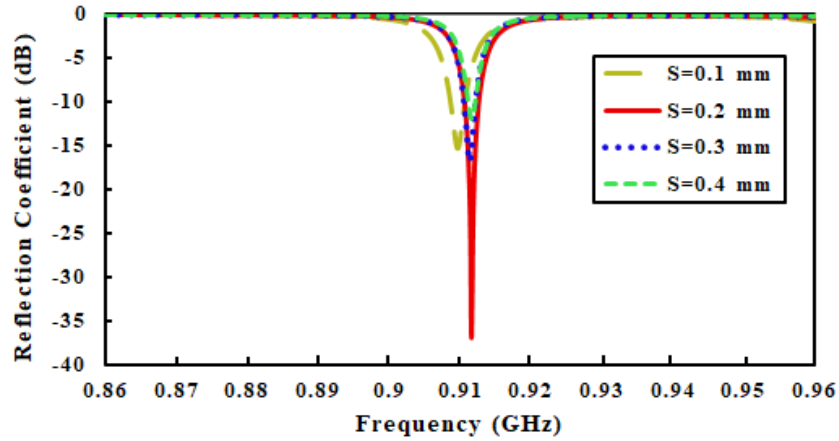


Figure 4.10 Simulated reflection coefficient response at different S values.

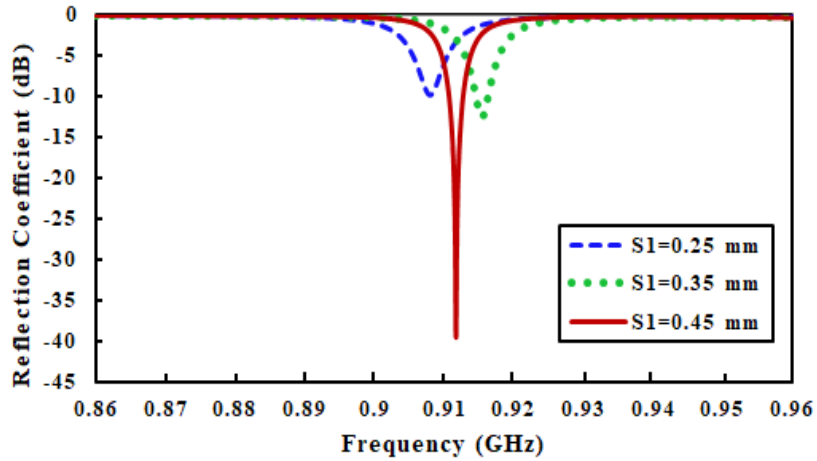


Figure 4.11 Simulated reflection coefficient response at different S₁ values.

The tag antenna design is implemented on a low-cost dielectric PTFE $55.80 \times 44 \text{ mm}^2$ substrate with a thickness of 1.43 mm. Increasing the open stubs number from three to seven at each side decreased the resonance frequency from 2.86 GHz to 912 MHz. By varying the

open stub length from 11.5 mm to 15.5 mm the resonance frequency shifted down from 1.06 GHz to 912 MHz at a rate of 39 MHz/mm. Increasing the width of the open stubs (W) decreased the resonance frequency from 984 MHz to 912 MHz at a rate of 72 MHz/mm. By adjusting the gaps between the nested open stubs (A), (S) and (S₁), the reflection coefficient S₁₁ value of -39.56 dB is achieved. The Simulation results are presented in the next chapter.

Chapter 5

Simulation Results and Discussion

Chapter Five

Simulation Results and Discussion

In order to evaluate the proposed tag antenna performance, S_{11} , VSWR, gain, directivity, radiation pattern, realized gain and read range are all investigated in this chapter. RFID technology is used in various metal-mounted applications thus, the effect of the back metal plate is studied by varying its dimensions. The effect of the back metallic plate dimensions on the realized gain, read range and radiation pattern are presented. Furthermore, RFID used is non-limited to metal-mountable applications only where RFID technology is used in very wide fields where the tag is mounted on different materials. Therefore, the proposed tag antenna is mounted on different dielectric plates and its performance is compared with placing it on metal in terms of realized gain, read range and radiation pattern.

5.1 Simulation Results

To verify the proposed design performance, fundamental parameters are studied such as reflection coefficient (S_{11}), VSWR, antenna gain, radiation pattern, directivity, realized gain and read range.

First, the simulation results of the proposed tag antenna placed on $20 \times 20 \text{ cm}^2$ a perfect conductor (PEC) plate are presented .

5.1.1 Reflection Coefficient S_{11} and VSWR

Figure 5.1 shows the reflection coefficient S_{11} in dB.

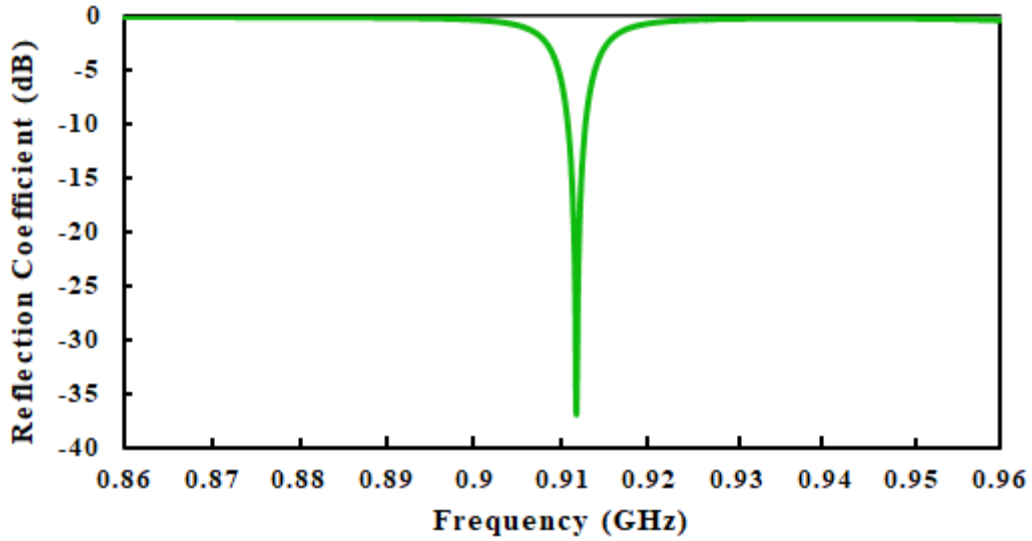


Figure 5.1 S-parameter of the proposed tag antenna.

It is noticed that the S_{11} is -39.6 dB (less than -10 dB), where the proposed design has a significant response at the resonance frequency of 912 MHz. Moreover, the VSWR is almost unity (VSWR= 1.2) at the resonance frequency as shown in Figure 5.2 which means realizing optimal impedance matching between the tag antenna and the IC chip.

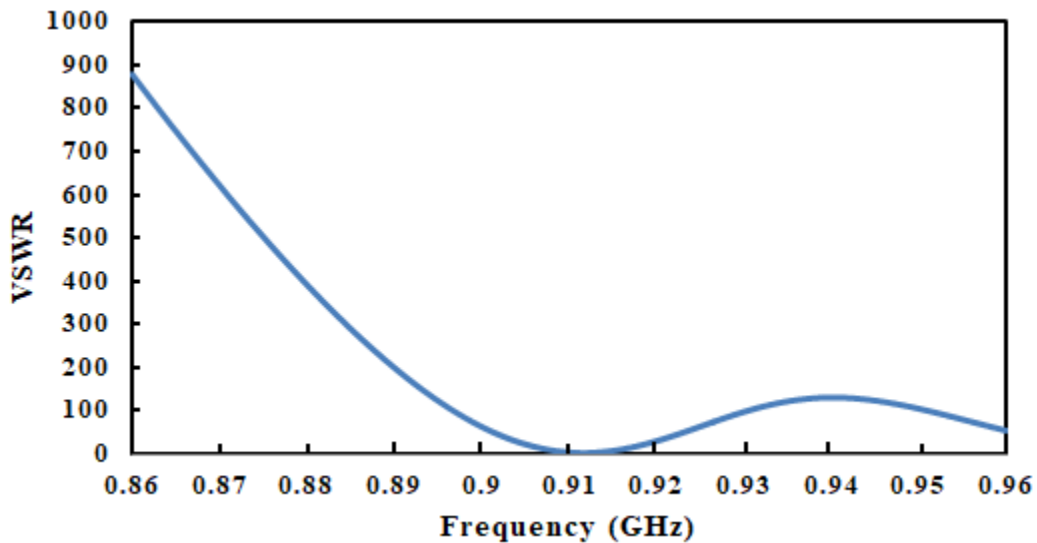


Figure 5.2 VSWR of the proposed RFID tag antenna over UHF band.

5.1.2 Radiation Pattern

The proposed tag antenna polar and 3D radiation pattern at the resonance frequency of 912 MHz is illustrated in Figure 5.3 (a) and (b) respectively.

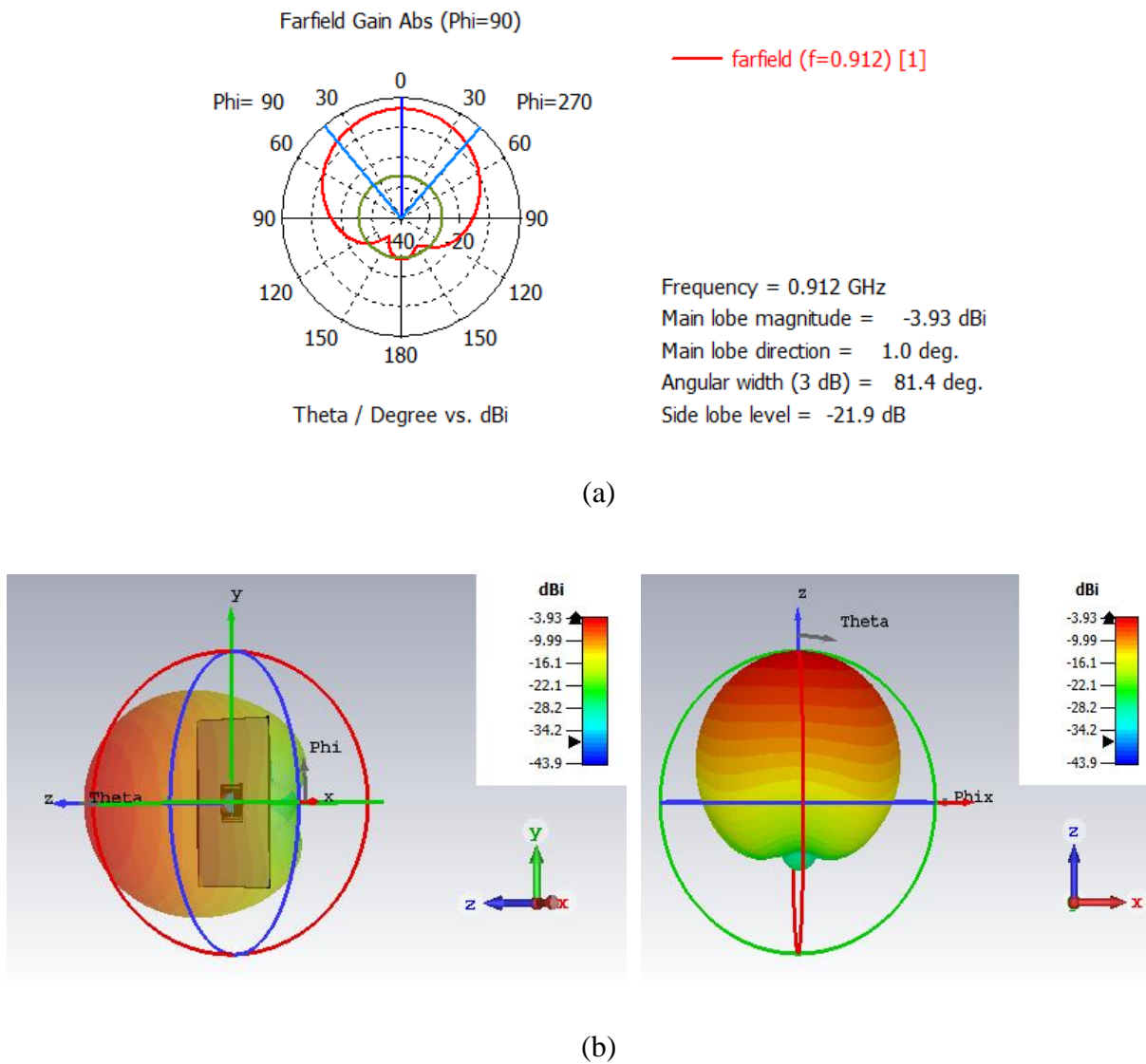


Figure 5.3 Radiation pattern of the RFID tag antenna at the resonance frequency 912 MHz (a) polar radiation pattern (b) 3D radiation pattern.

The radiation pattern shows how the back metallic object acts as a reflector. The metallic plate reduces the tag antenna back radiation, therefore enhances the tag performance. Whereby placing the tag on the metallic plate enhances the antenna gain and directivity compared to the tag performance in free space.

5.1.3 Gain and Directivity

The simulated tag antenna gain and directivity in free space and when placed on $200 \times 200 \text{ mm}^2$ metallic plate are represented in Figure 5.4 and Figure 5.5 respectively.

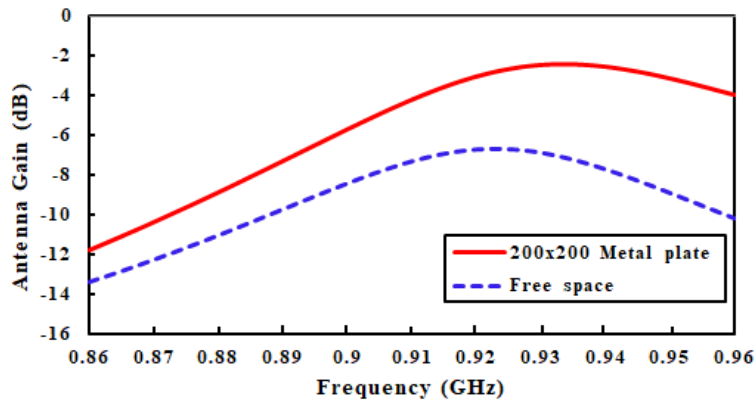


Figure 5.4 Simulated gain of the presented RFID tag antenna placed on $200 \times 200 \text{ mm}^2$ metal plate and in free space.

The tag antenna mounted on $200 \times 200 \text{ mm}^2$ metal plate gain is -3.93 dB at its resonance frequency of 912 MHz. Besides, the tag antenna has almost a constant directivity over the UHF band (7.36 dB). Whereas the antenna gain is -7.13 dB and the directivity is 3.24 dB in free space. The results show how placing the tag on the metallic plate enhances its performance.

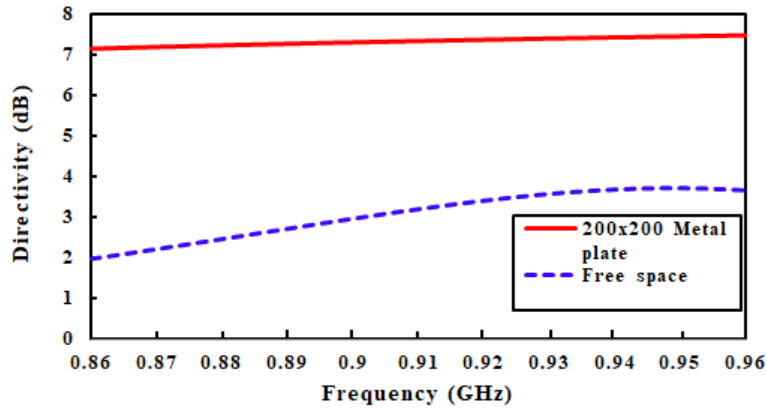


Figure 5.5 The directivity of the proposed RFID tag antenna placed on $200 \times 200 \text{ mm}^2$ metal plate and at free space.

5.1.4 Realized Gain

Realized gain and read range are important parameters to evaluate the tag antenna performance.

Figure 5.6 shows the simulated realized gain of the presented RFID tag antenna design.

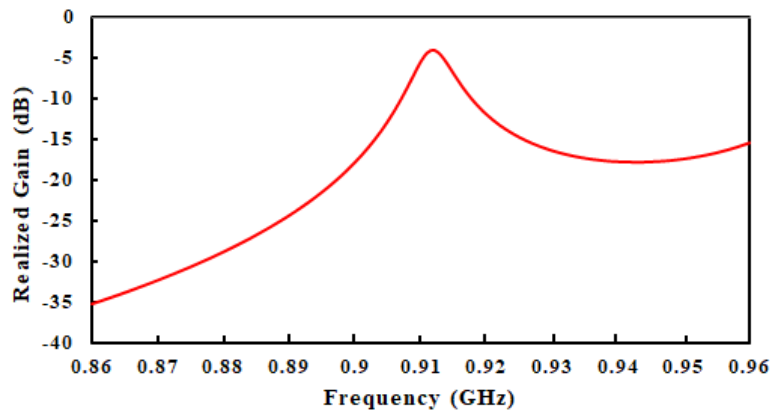


Figure 5.6 The realized gain of the proposed tag antenna.

The result show that the realized gain peak is -3.97 dB at the resonance frequency 912 MHz . The maximum realized gain value is $> -10 \text{ dB}$ which is acceptable to achieve a sufficient read range.

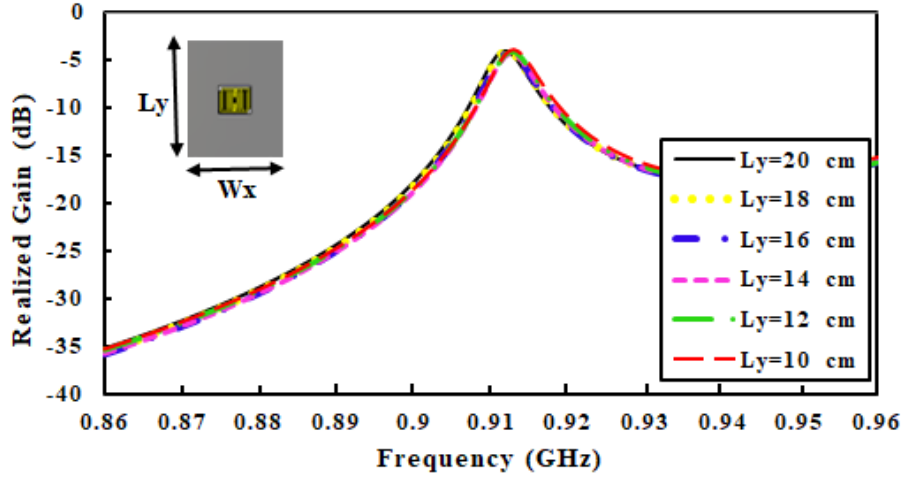
5.1.5 Read Range

In order to calculate the read range Friis formula is used; $r = (\lambda/4\pi) \sqrt{\frac{P_{EIRP} \times G_r}{P_{th}}}$, where $\lambda = 0.3289$ m at 912 MHz, $P_{EIRP} = 4$ W, $G_r = -3.97$ dB, $P_{th} = -20.5$ dBm.

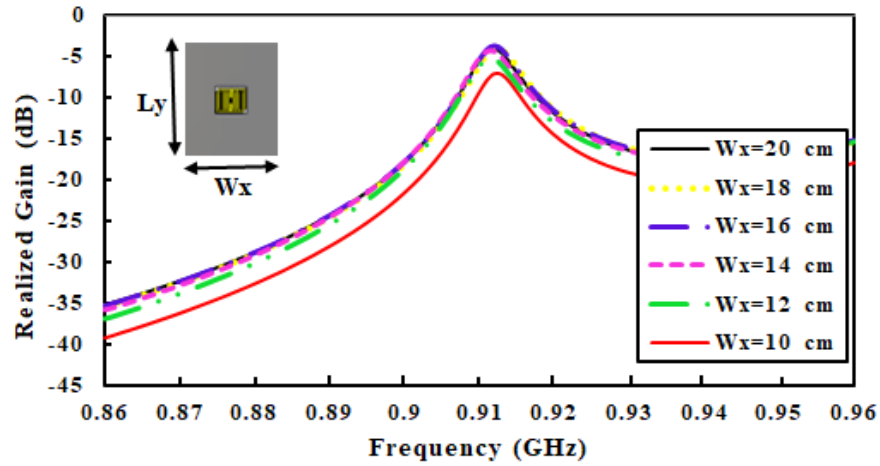
The computed read range $r = 11.104$ m, means that the RFID reader can detect the proposed tag placed on 200×200 mm² metallic object from distance up to 11.104 m.

5.2 Study of Back Metallic Object Effect

The effect of the back metallic plate on the proposed tag antenna performance is investigated through the realized gain. First, the metallic plate length L_y is varied from 10 cm to 20 cm while its width W_x is fixed at 20 cm. According to Figure 5.7(a), it is observed that varying L_y doesn't affect the realized gain much, therefore the read range of all cases nearly 11.104 m. Then, W_x is changed from 10 cm to 20 cm while L_y is fixed at 20 cm. According to Figure 5.7(b), the realized gain decreased to -7.1 dB when W_x is decreased to 10 cm whereby the read range is affected. The computed read range according to the simulated realized gain of each case of varying W_x is shown in Table 5.1.



(a)



(b)

Figure 5.7 Simulated realized gain of the proposed tag antenna for the metal plate with different

(a) plate length L_y and (b) plate width W_x .

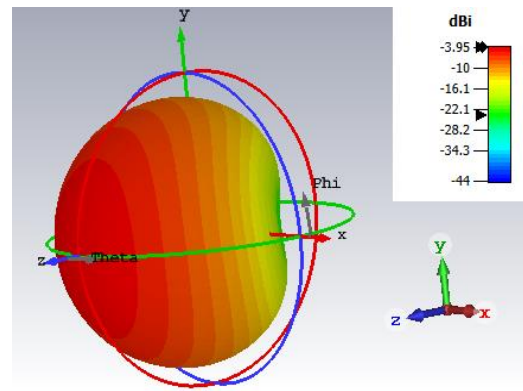
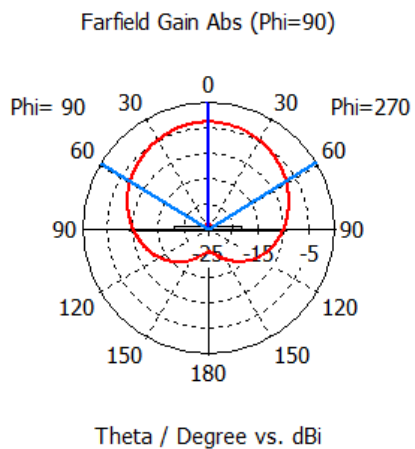
The read range is decreased to 7.8 m when the tag is mounted on a metal plate with a width of $W_x = 10$ cm. This is because of the electrical flux strength at $\theta = 0^\circ$ which affects the read range with tuning the back metal plate width W_x but not affected by the variation of the length L_y [8]. Similar performance degradation is observed in [8] where the tag antenna read range decreased by 4 meters due to variation of the metallic plate width from 20 cm to 10 cm with a fixed length of 20 cm.

Table 5.1 Simulated resonant frequency, realized gain and computed read range of the proposed tag antenna mounted on a metal plate has fixed length ($L_y = 20$ cm) and varying width (W_x).

Metal Plate (W_x cm \times L_y cm)	Resonant Frequency f (MHz)	Realized Gain Gr (dB)	Read range r (m)
10 \times 20	912.3	-7.02	7.81
12 \times 20	911	-5.22	9.63
14 \times 20	911	-4.29	10.71
16 \times 20	912	-3.64	11.53
18 \times 20	912	-3.93	11.16
20 \times 20	912	-3.97	11.10

The radiation patterns of the proposed tag antenna mounted on 20×10 cm² and 10×20 cm² metal plate at the resonance frequency are shown in Figure 5.8 and Figure 5.9 respectively.

It can be seen that the radiation pattern changed when the tag is mounted on a 10×20 cm² metal plate, unlike the 20×10 cm² metal plate which has almost the same radiation pattern of 20×20 cm² case.



(a)

(b)

Figure 5.8 The radiation pattern of the presented tag antenna mounted on $20 \times 10 \text{ cm}^2$ (a) polar radiation pattern, (b) 3D radiation pattern.

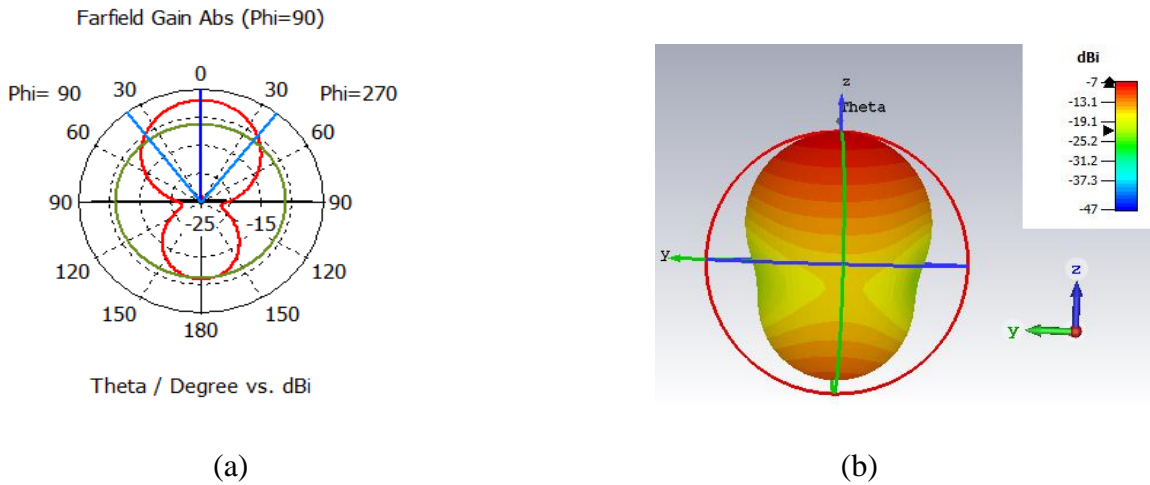


Figure 5.9 The radiation pattern of the presented tag antenna mounted on $10 \times 20 \text{ cm}^2$ (a) polar radiation pattern, (b) 3D radiation pattern.

It is worth mentioning that the resonant frequency of the presented tag antenna is not affected much by varying the back metal plate dimensions which is a preferable feature when designing a tag antenna for RFID metal-mountable applications.

5.3 The Proposed RFID Tag Antenna Mounted on Non-Metallic Objects

In this section, the presented tag antenna is mounted on various back dielectric plates to study the tag antenna performance through the simulated realized gain and computed read range. The proposed tag is placed on $20 \times 20 \text{ cm}^2$ glass, paper and Polycarbonate plates respectively. The realized gain of the tag antenna placed on different dielectric plates is shown in Figure 5.10, the resonance frequency is decreased by 3 MHz when the tag is placed on the dielectric plates. The simulated realized gain and the computed read range are illustrated in Table 5.2.

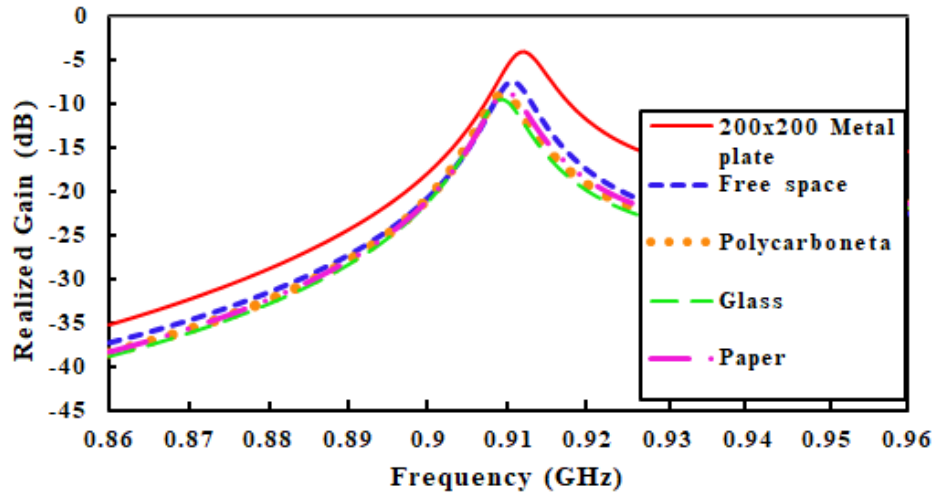


Figure 5.10 Simulated realized gain of the proposed tag antenna when it is placed on different dielectric $200 \times 200 \text{ mm}^2$ plates, metal plate and in free space.

The realized gain decreased when the tag antenna is placed on dielectric plates, thus the read range decreased too. The detection distance is 5.94 m on glass, 6.51 m on Polycarbonate and 6.29 on paper. The radiation pattern of the proposed tag antenna when mounted on $200 \times 200 \text{ mm}^2$ glass and Polycarbonate plate are shown in Figure 5.11 and Figure 5.12 respectively.

Table 5.2 simulated resonant frequencies, realized gain and computed read range of the proposed tag antenna mounted on $20 \times 20 \text{ cm}^2$ metallic and non-metallic plates.

Back object material (20×20) cm^2	Resonant Frequency f (MHz)	Realized Gain Gr (dB)	Read range r (m)
Metal (PEC)	912	-3.97	11.1
Polycarbonate 2.9	909	-8.93	6.29
Glass 6.4	909	-9.43	5.94
Paper 2.3	910	-8.63	6.51

Free space	911	-7.54	7.37
------------	-----	-------	------

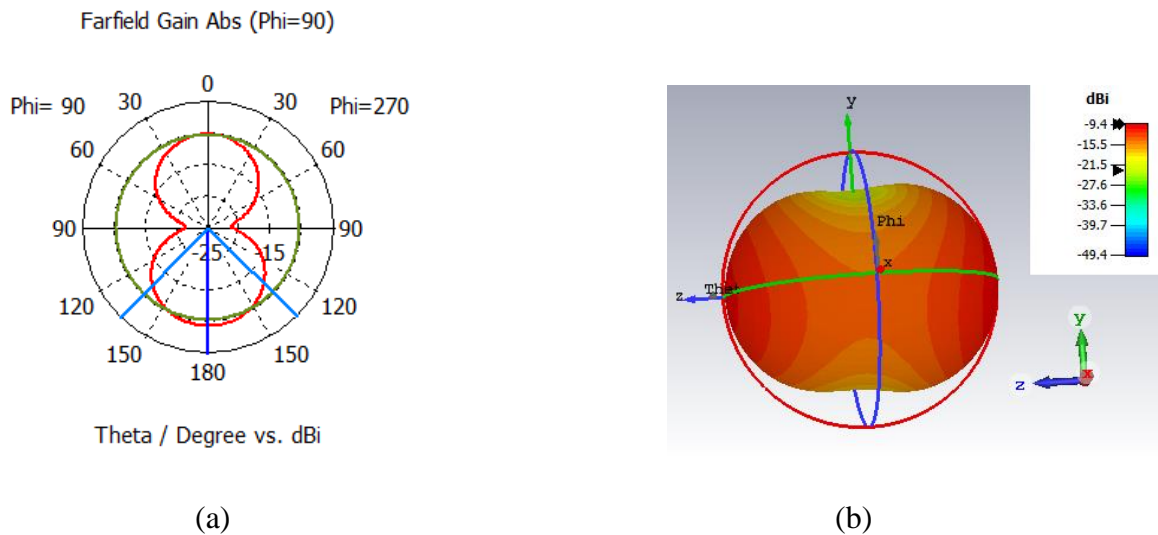


Figure 5.11 Radiation pattern of the RFID tag antenna placed on $200 \times 200 \text{ mm}^2$ glass plate at its resonance frequency (a) polar radiation pattern (b) 3D radiation pattern.

Radiation patterns of the tag antenna mounted on both glass and Polycarbonate plates are convergent and differs from the metallic plate. The metallic plate is a high reflector therefore; the tag antenna back radiation is much less than the case of the dielectric plates. Therefore, mounting the proposed tag antenna on a metallic plate enhances its performance.

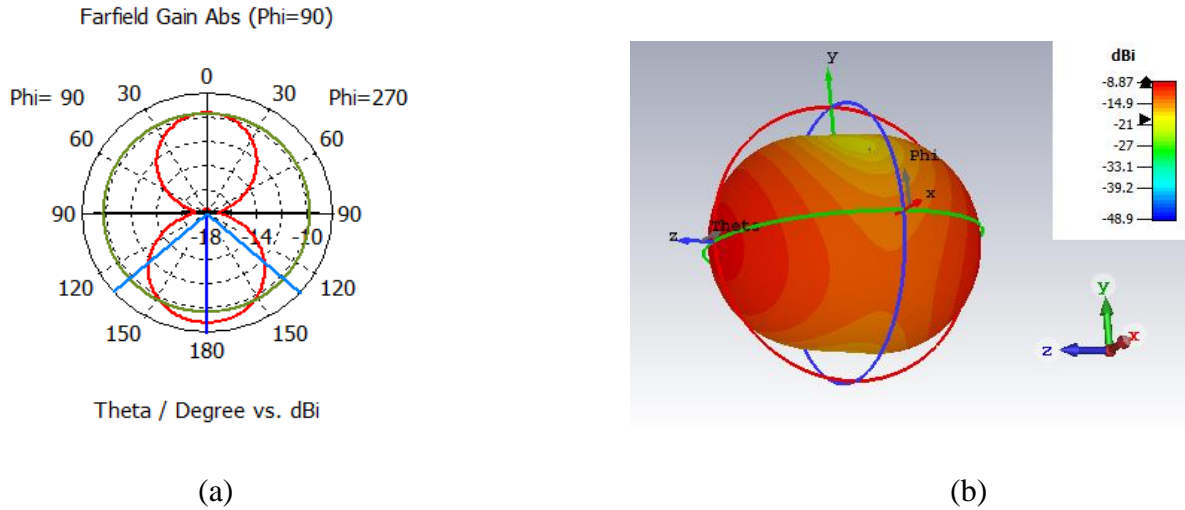


Figure 5.12 Radiation pattern of the RFID tag antenna placed on $200 \times 200 \text{ mm}^2$ Polycarbonate plate at its resonance frequency (a) polar radiation pattern (b) 3D radiation pattern.

The results show that the presented RFID tag antenna is detected from a distance up to 11.1 m while the tag antenna is mounted on a metal plate, and 6.51 m while the tag is placed on a dielectric one. Little fluctuation in the tag antenna resonance frequency is observed when it is placed on various metallic and dielectric plates thus; the proposed tag can be used for various metallic and non-metallic RFID applications.

5.4 Performance Comparison

Table 5.3 shows a comparison between this proposed tag antenna and previous published UHF RFID metal-mountable tag antennas. Multilayer tags are used in [9] and [13] each consists of two substrates and three conductive layers. The layers were loaded by using four vias [9] and two shorting stubs [13]. The structure thickness exceeded 2 mm besides using vias and stubs all increased the fabrication cost. The utilization of a double layer structure DLS-EBG structure as a ground of a dipole tag antenna in [12]. 5×1 DLS-EBG units are attached using 10 offset vias and

loaded below the dipole tag by 6 metallic screws. Although a higher read range was achieved, the structure is too bulky and required extra elements which increased the fabrication cost and complexity. A foam spacer with a 1 cm thickness between the tag antenna and the back metallic plate was used in [6] to overcome the back metal effect. Both [61] and [54] used two polarized inverted-F antenna PIFA elements. A dual-PIFAs placed in a cross configuration are shorted to the ground plane by 12 vias [61]. Feeding loops and radiators were etched on a 1 mm FR4 substrate and the whole tag was placed on a 3 mm thickness foam then shorted to the ground plane by two shorting strips [54]. Two radiated patches are shorted to the ground by 8 metallic vias via holes to form PIFA in [49], a T-matching and the ground plane are etched to the substrate which needed extra fabrication work thus, increased the cost. Compared to the reported works, the proposed design does not consist of any shorting elements like vias, stubs, strips or screws. The tag configuration has no requirement of any hard complex fabrication work like etching or drilling. The proposed tag antenna is implemented on a single-layer inexpensive PTFE substrate. Although [12],[13] and [6] achieved higher read range, their structures are much larger and have shorting elements which increases the cost and complexity. The proposed design is simple, single-layered, easy to fabricate, low profile and has low cost thus, it is convenient for mass production.

Table 5.3 Comparison between the proposed tag and previous published UHF RFID metal mountable tags.

Ref.	Tag Dimension (mm ³)	Shorting Elements	Chip Sensitivity (dBm)	Read Range (m)
[10]	50 × 55.55 × 1.6	No	-8	5.56
[9]	31 × 19.5 × 3.065	Vias	-8	4.7
[13]	40 × 40 × 3.087	Stubs	-18.5	14.3
[12]	72 × 32 × 6.8	Vias	-16	16
[6]	51 × 34 × 1.58	No	-8	4.5
[61]	64 × 64 × 2	Vias	-17	12
[49]	60 × 45 × 1.6	Vias	-19	6.2
[54]	50 × 50 × 4	Strip	-	5.50
[50]	38 × 38 × 1.6	Stubs	-17.8	6.77
This work	55.8 × 44 × 1.5	No	-20.5	11.1

The tag antenna placed on 200 × 200 mm² metal plate gain is -3.93 dB at a resonance frequency of 912 MHz and it has an almost constant directivity of 7.36 dB. The realized gain is -3.97 dB and the read range is up to 11.104m. While varying the metallic plate width (W_x), the read range decreased to 7.8 m but it is not affected by the variation of the metallic plate length (L_y). The

detection distance of the proposed design on different $200 \times 200 \text{ mm}^2$ dielectric plates is 5.94 m on glass, 6.51 m on Polycarbonate and 6.29 m on paper.

Chapter 6

Conclusion and Future Work

Chapter Six

Conclusion and Future Work

6.1 Conclusion

In this work, a novel compact single-layer metal-mountable UHF RFID tag antenna is proposed. The design is composed of nested identical open stubs forming U-shaped mutually coupled segments. The main antenna parameters such as the reflection coefficient, radiation pattern, gain, directivity, realized gain and read range are investigated. Tuning the resonance frequency and the impedance matching between the proposed tag antenna and the IC chip are realized by tuning the open stubs dimensions, number and stubs separation. Increasing the number of the open stubs with forming additional U- shaped segments increases the mutual coupling effect which provides a stronger radiation field thus, enhances the gain. The metallic plate reduces the tag antenna back radiation and increases the directivity of the tag antenna; therefore placing the proposed tag on the metallic plate enhances the tag antenna performance. The proposed tag antenna performance is not affected by varying the length of the metallic plate unlike varying the metallic plate width. The realized gain decreased by changing the width of the metallic plate due to the variation of the tag antenna radiation pattern. Moreover, the realized gain and the read range are decreased in the dielectric plate case compared to the metallic one. The dielectric plates do not reflect the incident wave, thus the back radiation increased. The computed read range was 11.104 m and 7.37 m when the tag was placed on a $20 \times 20 \text{ cm}^2$ metallic object and in free space respectively. Indeed, the read range was up to 6.51 m when the tag was mounted on a dielectric plate. A relatively high read range is achieved besides little fluctuation in the tag antenna resonance frequency is observed when the proposed tag antenna is mounted on various metallic and dielectric plates thus; the proposed

tag can be used for various metallic and non-metallic RFID applications. The proposed design provides a simple tuning mechanism, easy to fabricate and has a low cost. Thus, the design is convenient for mass production.

6.2 Future Work

- 1- Increase the identical open stubs number by adding two additional open stubs at each upper and lower side of the proposed antenna structure. Loading additional stubs increases the antenna inductance thus, decreases the resonance frequency. Moreover, increasing the number of the open stubs (forming additional U- shaped segments) increases the mutual coupling effect which provides stronger radiation field thus, realizes a higher gain as investigated in chapter 4. As the open stubs were increased from 5 to 7 in this work, the resonance frequency was 912 MHz. Hence, by loading the additional open stubs the frequency will be lower than the required band. Therefore, you have to reduce the structure dimensions to increase the resonance frequency. Thus, you will be able to minimize the tag size.
- 2- Investigate the effect of adding open stubs with different lengths instead of using identical open stubs as proposed in this work. Tune the lengths of the open stubs to achieve a wide band covers the entire UHF RFID band (860-960 MHz), whereby UHF RFID frequency regulations around the world is within this band (860- 960 MHz) Thus, the design can be used worldwide without the requirement of readjusting the antenna parameters to tune the operation frequency.
- 3- Using a full copper ground plane lead to narrow the operation frequency band as it resulted in the proposed work. Remove the copper ground plane and retune the design parameters to achieve a wide frequency band to cover the entire UHF RFID band (860-

960 MHz). Applying the tag antenna without the ground plane on the metallic plate necessitates separating the tag antenna substrate and the back metallic plate by an air gap. Consider tuning the thickness of the air gap through the optimization.

References

- [1] Kamran Ahsan, "RFID Components, Applications and System Integration with Healthcare Perspective," in *Deploying RFID - Challenges, Solutions, and Open Issues.*: InTech, 2011.
- [2] J. Uddin et al., "UHF RFID antenna architectures and applications," *Scientific Research and Essays Vol. 5(10)*, pp. 1033-1051, 2010.
- [3] P. Cole, "A Study of Factors Affecting the Design of EPC Antennas & Readers for Supermarket Shelves," 2002.
- [4] Manish Bhuptani and Shahram Moradpour, *RFID Field Guide: Deploying Radio Frequency Identification Systems.*, 2005.
- [5] Shin-Rou Lee, Eng-Hock Lim, Fwee-Leong Bong, and Boon-Kuan Chung, "Slotted Circular Patch with Multiple Loading Stubs for Platform Insensitive Tag," *IEEE Transactions on Antennas and Propagation*, 2018.
- [6] Mohammed Ali Ennasar, Ikram Aznabet, Otman El Mrabet, and Mohamed Essaaidi, "Design and Characterization of a Compact Single Layer Modified S-Shaped Tag Antenna for UHF-RFID Applications," *Advanced Electromagnetics 8(1)*, pp. 59-65, 2019.
- [7] Fuad Erman et al., "Low-profile folded dipole UHF RFID tag antenna with outer strip lines for metal mounting application," *Turkish Journal of Electrical Engineering & Computer Sciences*, 2020.

- [8] Fuad Naim Ahmed Erman et al., "U-Shaped Inductively Coupled Feed UHF RFID Tag Antenna with Defected Microstrip Surface for Metal Objects," *IEEE Antennas and Wireless Propagation Letters*, 2020.
- [9] Karrar Naji Salman, Alyani Ismail, Raja Syamsul Azmir Raja Abdullah, and Tale Saeedi," Coplanar UHF RFID tag antenna with U-shaped inductively coupled feed for metallic applications", *PLoS ONE 12(6)*, 2017. [https:// doi.org/10.1371/journal.pone.0178388](https://doi.org/10.1371/journal.pone.0178388).
- [10] Adam R. H. Alhawari et al., "Omega-Shaped Tag Antenna with Inductively-Coupled Feeding Using U-Shaped Stepped-Impedance Resonators for RFID Applications," *Applied Computational Electromagnetics Society Journal 35(8)*, pp. 951-959, Oct 2020.
- [11] Md. Rokunuzzaman and Mohammad Tariqul Islam, "Design and Experimental Evaluation of Modified Square Loop Feeding for UHF RFID Tags," *PLoS ONE 10(7)*, 2015.
- [12] Xiuping Li et al., "A Novel UHF RFID tag antenna based on the DLS-EBG Structure for Metallic Objects," *IET Microwaves Antennas & Propagation 14(7)*, pp. 567-572, 2020.
- [13] Yaw-Hua Niew, Kim-Yee Lee, Eng-Hock Lim, Fwee-Leong Bong, and Boon-Kuan Chung, "Patch-loaded Semicircular Dipolar Antenna for Metal-Mountable UHF RFID Tag Design," *IEEE Transactions on Antennas and Propagation*, 2019.
- [14] Klaus Finkenzeller, *RFID Handbook: Fundamentals and Applications in Contactless Smart Cards and Identification, 2nd Edition.*, 2003.

- [15] Pedro Sebastián Gómez Meneses, *Extremal Optimisation Applied to Constrained Combinatorial Multi-Objective Optimisation Problems*, 2012.
- [16] Paulo Crepaldi and Tales Pimenta, "Introductory Chapter: RFID: A Successful History," in *Radio Frequency Identification*.: InTech, 2017.
- [17] Jeremy Landt, "The history of RFID," *IEEE Potentials*, 2005. DOI: 10.1109/MP.2005.1549751.
- [18] Alfred Koelle, Steven Depp, and Robert Freyman, "Short-Range Radio-Telemetry for Electronic Identification Using Modulated Backscatter," *Proceedings of the IEEE*, pp. 1260-1261, 1975.
- [19] Hongtao Song, Haibo Liu, and Haiyan Lan, "2.4GHz Active RFID System Based on nRF24LE1," *IEEE*, 2011.
- [20] Ernest Arendarenko and Teemu H. Laine, "Smart tagging technologies in pervasive learning environments", 2011.
- [21] V. Daniel Hunt, Albert Puglia, and Mike Puglia, *RFID: A Guide to Radio Frequency Identification*.: WILEY, 2007.
- [22] Paul Sanghera, *RFID+ Study Guide and Practice Exam*.: Syngress Publishing, 2007.
- [23] (2012, November) Regulatory status for using RFID in the UHF spectrum. [Online]. <https://gs1it.org/>. Accessed on: October 20, 2020.

- [24] Rajiv Anand. (2018, November) Global frequency regulations for RFID. [Online]. <https://tagitsolutions.com>. Accessed on: October 20, 2020.
- [25] Peter. H. Cole, Zhonghao Hu, and Yuexian Wang, "Operating Range Evaluation of RFID Systems," in *Advanced Radio Frequency Identification Design and Applications.*: InTech, 2011.
- [26] Gerarg Zamora Gonzalez, "Radio Frequency Identification (RFID) Tags and Reader Antennas Based on Conjugate Matching and Metamaterial Concepts," *Bellatera*, p. 18, 2013.
- [27] Mun Leng Ng, "Design of High Performance RFID Systems for Metallic Item Identification," *The University of Adelaide, Australia letters*, 2008.
- [28] SHENZHEN XINYETONG TECHNOLOGY DEVELOPMENT CO.,LTD. [Online]. <https://www.asiarfid.com>. Accessed on: January 15, 2021.
- [29] Bahiru Shifaw, "Automated Classroom Monitoring With IOT and Virtuino App," *International Journal of Advanced Research in IT and Engineering* , 2019.
- [30] Simson Garfinkel and Henry Holtzman, "Understanding RFID Technology," in *RFID Technology.*: garfinkel.book, 2005, pp. 15-22.
- [31] Roy Want, "An Introduction to RFID Technology," IEEE CS and IEEE ComSoc, 2006.
- [32] Linda Castro and Samuel Fosso Wamba, "An Inside Look at RFID Technology," *Journal of Technology Management and Innovation*, 2007.

- [33] What is RFID? | The Beginner's Guide to RFID Systems. [Online]. <https://www.atlasrfidstore.com>. Accessed on: April 13, 2021.
- [34] K. V. Seshagiri Rao, Pavel V. Nikitin, and Sander F. Lam, "Antenna Design for UHF RFID Tags:A Review and a Practical Application," *IEEE Transection on Antennas and Propagations*, VOL. 53, NO. 12, pp. 3870-3876, 2005.
- [35] Warren L. Stutzman and Gary A. Thiele, *Antenna Theory and Design*, Third Edition.: John Wiley & Sons, Inc., 2012.
- [36] Constantine A. Balanis, *Antenna Theory Analysis and Design.:* A JOHN WILEY & SONS, INC., 2005.
- [37] Antennas Lecture two. [Online]. <https://feng.stafpu.bu.edu.eg>. Accessed on: July 1, 2021.
- [38] Fuad Erman et al., "Miniature Compact Folded Dipole for Metal," *electronics*, 2019.
- [39] BONG FWEE LEONG, "DESIGN AND CHARACTERIZATION OF MINIATURIZED ,"
Universiti Tunku Abdul Rahman letters, p. 19, 2017.
- [40] D. K. Naji, J. S. Aziz, and R. S. Fayath, "Design of Miniaturized Fractal RFID Tag Antenna with Forced Impedance Matching," *International Journal of Electromagnetics and Applications*, 2(5), pp. 129-139, 2012.
- [41] Bohan Zhang et al., "Flexible Anti-Metal RFID Tag Antenna Based on High-Conductivity Graphene Assembly Film," *Sensors*, 2021.

- [42] Muhammad Hussain, Yasar Amin, and Kyung-Geun Lee, "A Compact and Flexible UHF RFID Tag Antenna for Massive IoT Devices in 5G System," *Sensors*, 2020.
- [43] Johnny Lienau. (2019, Feb) Understanding Antenna Design. [Online]. www.lairdconnect.com. Accessed on: February 7, 2021.
- [44] (2021, July) Dig Deep – Construction of RFID Tags. [Online]. <https://rfid4u.com>. Accessed on: July 7, 2021.
- [45] Shahid Mansuri. (2019, Feb) Complete Guide to RFID: Benefits, Applications, and Challenges. [Online]. <https://dzone.com>. Accessed on: May 3, 2021.
- [46] Gaetano Marrocco, "The art of UHF RFID antenna design: impedance matching and size-reduction techniques," *IEEE Antennas and Propagation, Vo.50, N.1*, Jan 2008.
- [47] Adam Alhawari, Alyani Ismail, Ali ASadeq Abdulhadi Jalal, and Raja Syamsul Azmir Raja Abdullah, "U-Shaped Inductively Coupled Feed Radio Frequency Identification Tag Antennas for Gain Enhancement," *Electromagnetics 34(6)*, 2014.
- [48] Antenna Theory - Half-Wave Folded Dipole. tutorialspoint. [Online]. www.tutorialspoint.com. Accessed on: July 4, 2021.
- [49] Wenbo Zeng, Jia Zhao, Baozhong Ke, and Qiqi Wu, "Compact Microstrip RFID Tag Antenna Mountable on Metallic Objects," *Procedia Engineering 16*, pp. 320-324, 2011.

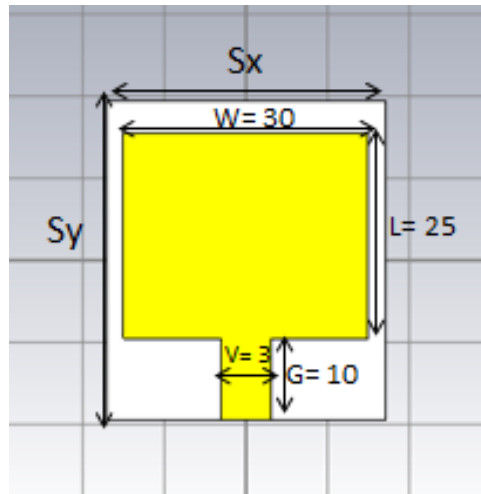
- [50] Shin-Rou Lee, Wai-Hau Ng, Eng-Hock Lim, Fwee-Leong Bong, and Boon-Kuan Chung, "Compact Magnetic Loop Antenna for Omnidirectional On-metal UHF Tag Design," *IEEE Transactions on Antennas and Propagation*, 2019.
- [51] S. Drabowitch, A. Papiernik, H. D. Griffiths, J. Encinas, and B. L. Smith, "Fundamentals of Electromagnetism," in *Modern Antennas Secoen Edition.*: Springer, 2005, ch. 1, pp. 7-14.
- [52] Mun Leng Ng, "Design of High Performance RFID Systems for Metallic Item Identification," *The University of Adelaide, Australia*, pp. 23-25, 2003.
- [53] María Elena De Cos and Fernando Las-Heras, "Troubleshooting RFID Tags Problems with Metallic," in *Current Trends and Challenges in RFID.*: InTech, 2011, ch. 9, pp. 171-186.
- [54] Byeongwi Mun, Yonghyun Yoon, Hyunwoo Lee, Hark-Yong Lee, and Byungje Lee, "A Compact Dual-Band RFID Tag Antenna Mountable on Metallic Objects," *International Journal of Antennas and Propagation*, 2015.
- [55] Mustafa Murat B'ILG'IC and Korkut YEG'IN, "An HF/UHF dual mode RFID transponder antenna and HF range extension using UHF wireless power transmission," *Turkish Journal of Electrical Engineering & Computer Sciences*, pp. 3949 – 3960, 2016.
- [56] Abdelaziz Hamani, Mustapha C. E. Yagoub, Tan-Phu Vuong, and Rachida Touhami, "A Novel Broadband Antenna Design for UHF RFID Tags on Metallic Surface

- Environments," *IEEE Antennas and Wireless Propagation Letters* (Vol: 16), pp. 91-94, 2016.
- [57] (23-Oct-2020) ALIEN, Higgs 4. [Online]. www.alientechnology.com. Accessed on: September 15, 2020
- [58] A. Bondeson, T. Rylander, and P. Ingelstrom, *Computational Electromagnetics.:* Springer, 2005.
- [59] Rose Hulman. (2007, Sep) CST MICROWAVE STUDIO® 2008 – Workflow and Solver Overview. [Online]. www.rose-hulman.edu. Accessed on: August 2, 2020.
- [60] Alien Technology Corporation. (2012, March) Alien Technology. [Online]. www.dcp.nl. Accessed on: September 15, 2020.
- [61] E.-S. Yang and H.-W. Son, "Dual-polarised metal-mountable UHF RFID tag antenna for polarisation diversity," *Electronic Letters*, 2016.

Appendix A

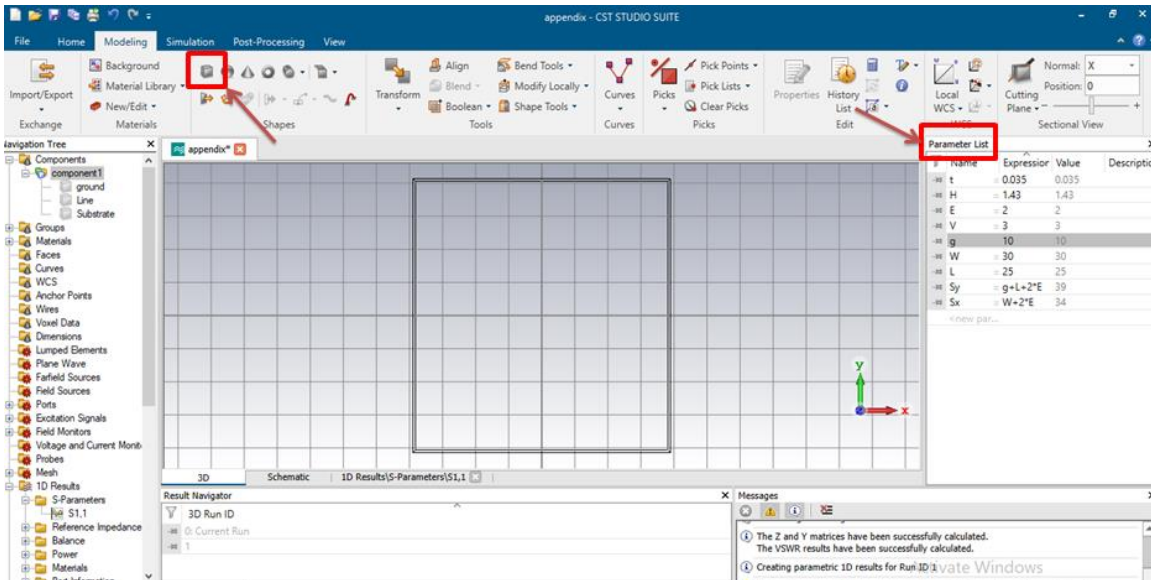
Simulation of the following tag antenna structure by CST Microwave Studio:

The substrate thickness is $H= 1.43$ mm, the thickness of the copper layer is $t= 0.035$ mm, all parameters in mm. The substrate material is PTFE.

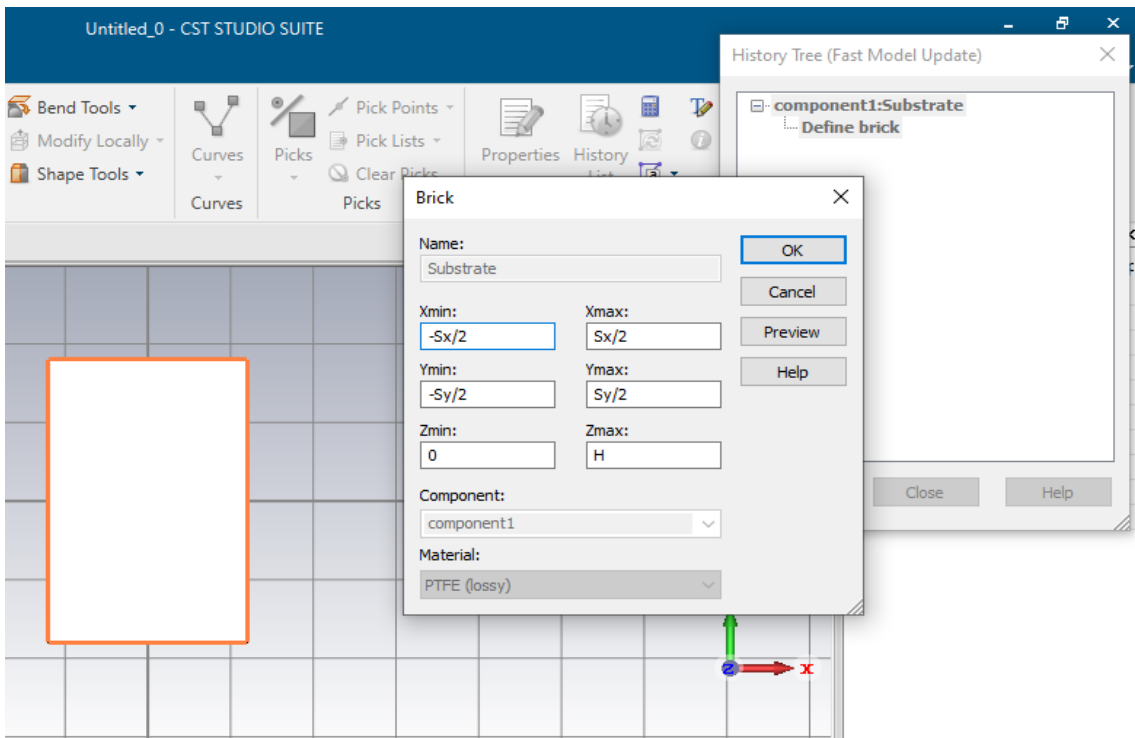


Geometric Construction Steps:

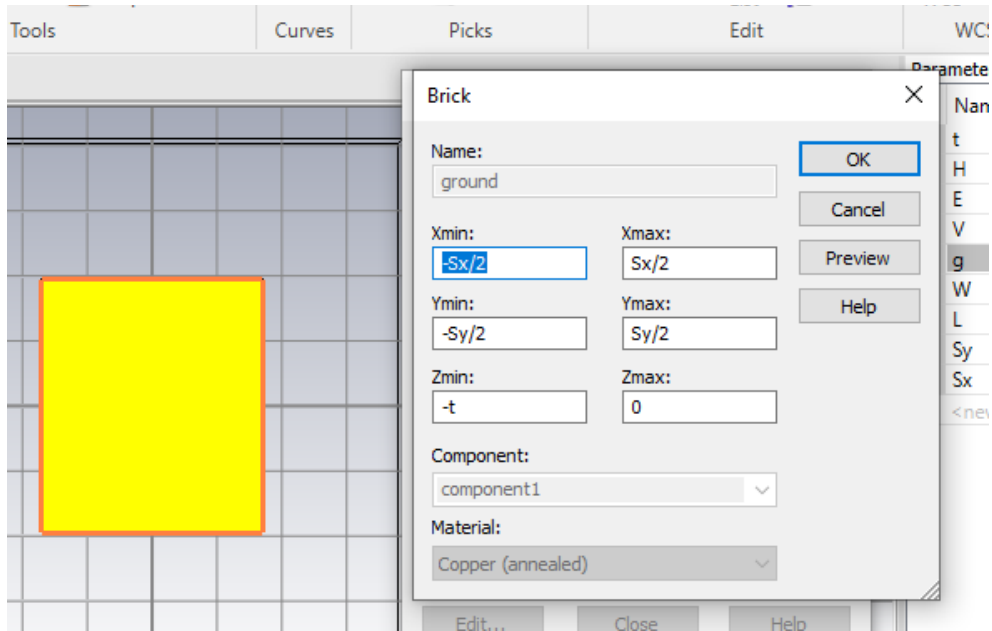
- Enter the parameters and parameters' values in the parameters list as shown in the following figure. Then, select the brick shape tool from the toolbar to create the substrate.



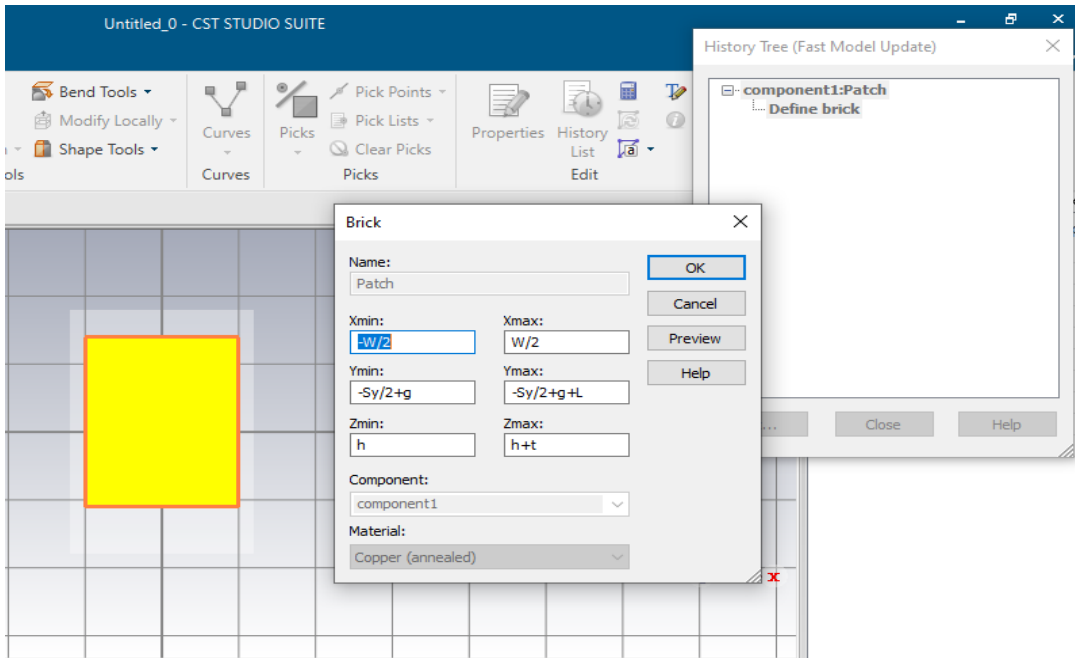
- Press ESC to bring up the brick window. Rename the brick shape to “substrate”. Enter the substrate width (Xmin, Xmax), length (Ymin, Ymax) and height (Zmin, Zmax) as shown in the figure below. Next, select the substrate material (PTFE Lossy) from the drop down menu in the brick window.



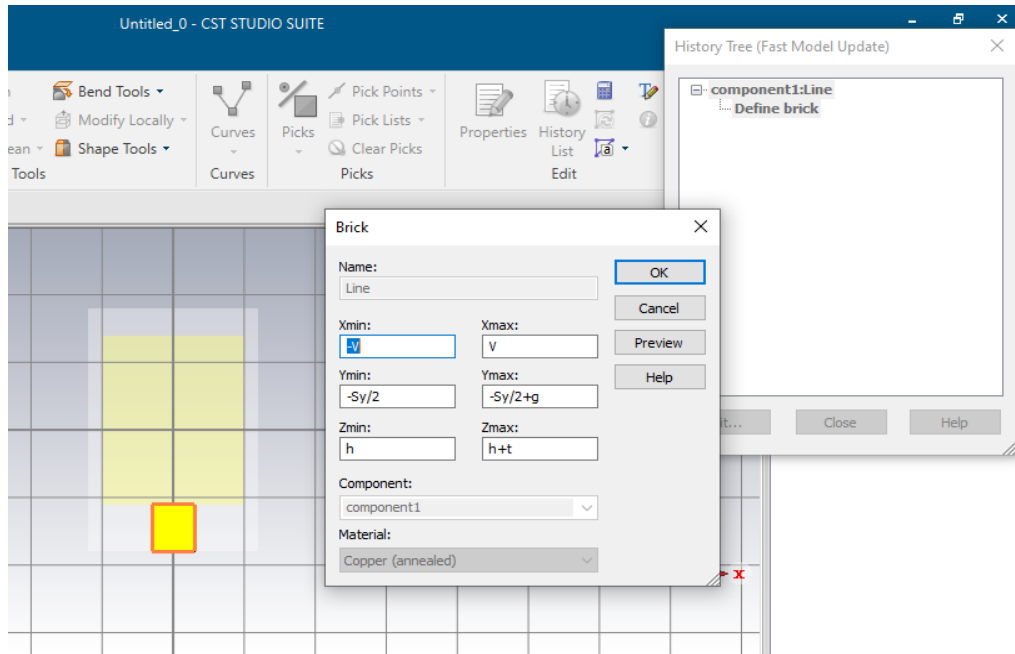
- Add the ground plane at the bottom side of the substrate. Select the brick shape and press ESC. Rename the brick to “Ground”. Enter the substrate width (Xmin, Xmax) and length (Ymin, Ymax) then, enter the copper layer thickness (-t) at Zmin as shown in the figure below. Select the ground material (Copper annealed) from the material section.



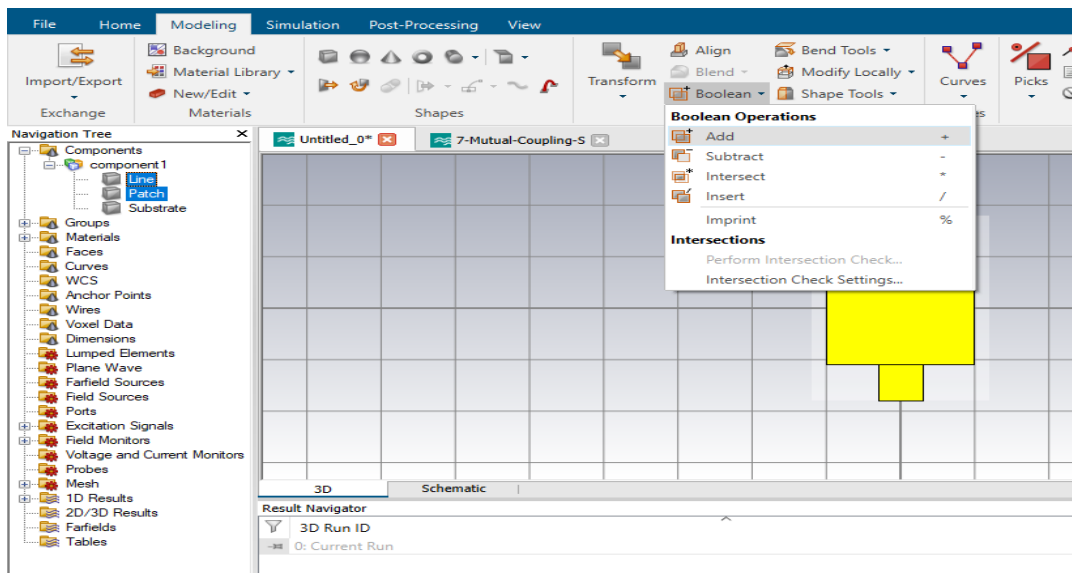
- To create the patch select the brick shape and press ESC. Rename the brick to “Patch”. Enter the patch dimensions as shown in the figure below. Select the patch material (Copper annealed).



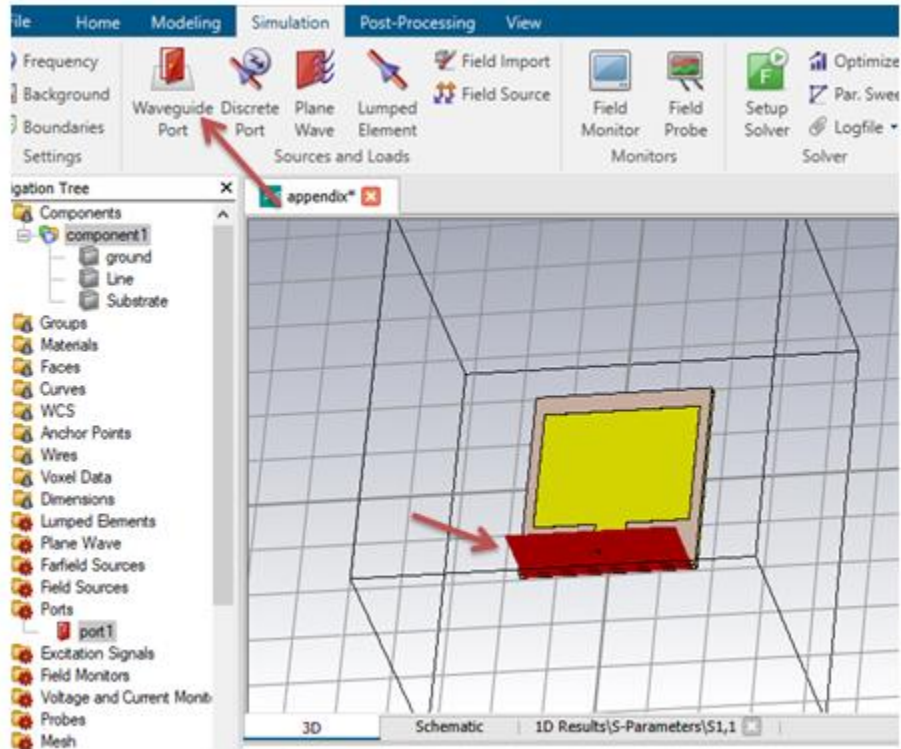
- To create the feeding line select the brick shape and press ESC. Rename the brick to “Line”. Enter the line dimensions at each as shown in the figure below. Select the line material (Copper annealed).



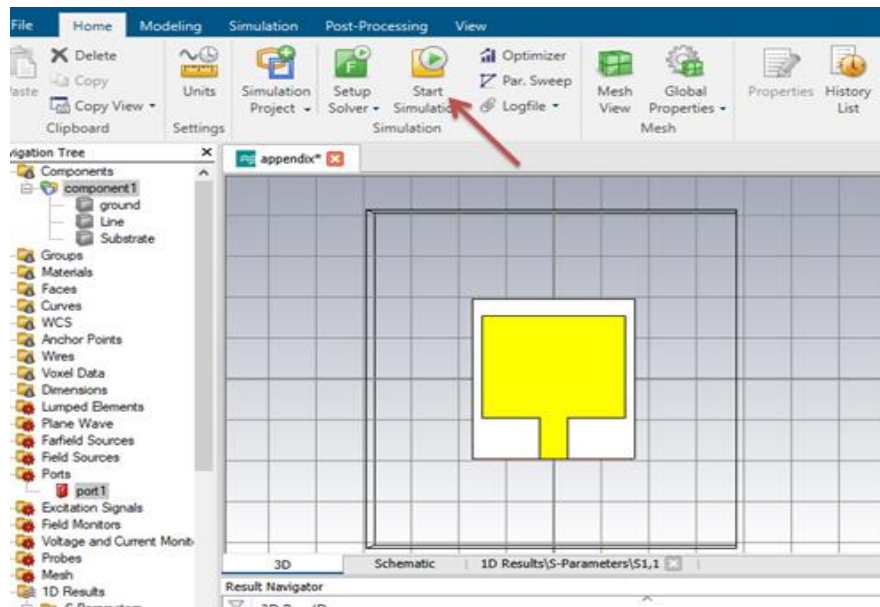
- Combine the antenna patch with the line. Press “ctrl” from the keyboard then, select both the patch and the line from “components” at the navigation tree. Press “add” from the “Boolean” tool as shown in the figure below.



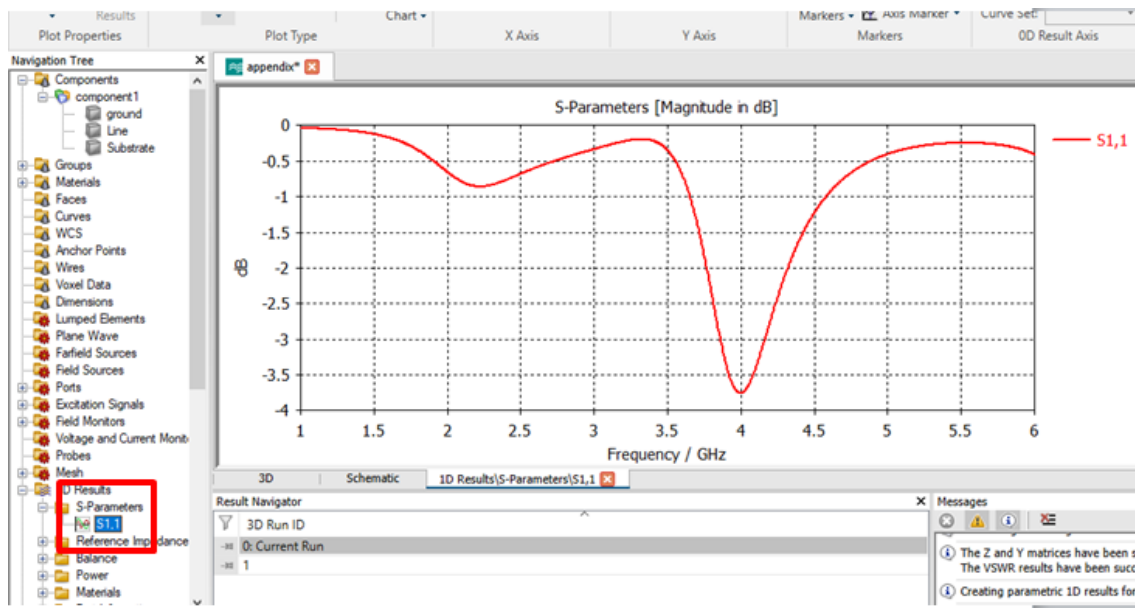
- To add an excitation port select the feeding line surface terminal then, select the port from the toolbar as shown in the figures below.



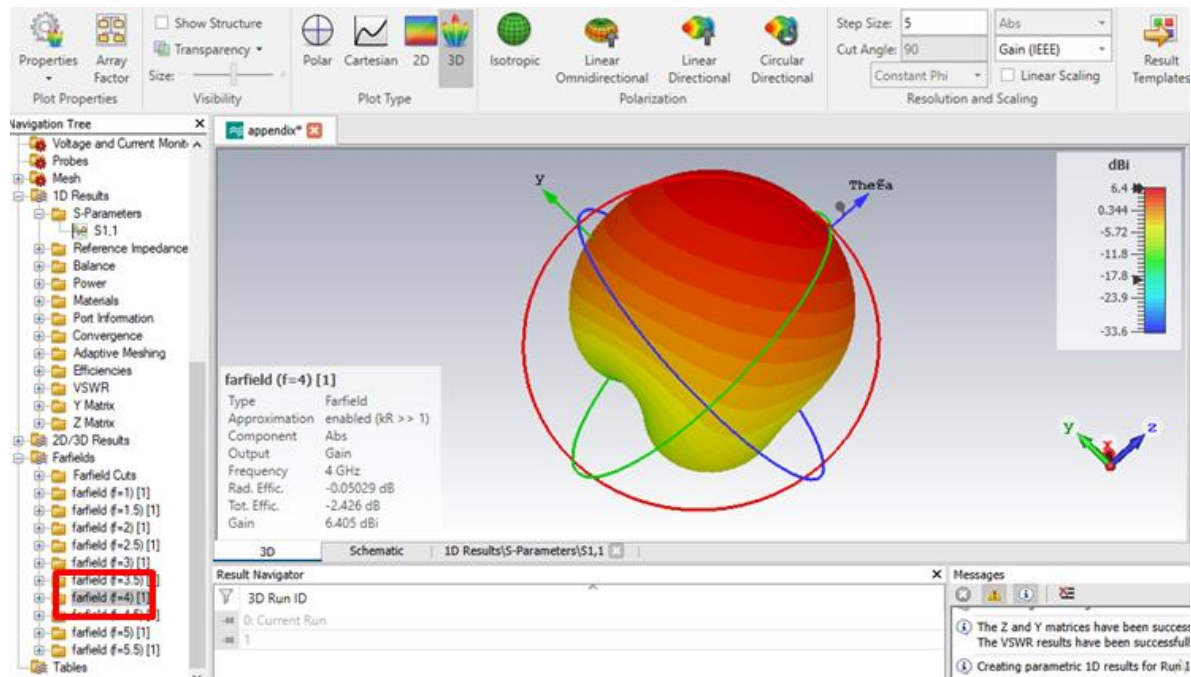
- The design is ready. To run the simulation press “Start simulation”.



- After the end of the simulation explore the simulation results at the navigation tree. Investigate the S- parameter from 1D Results folder as shown in the figure below.



- Investigate the radiation pattern at the resonance frequency from “Farfields” folder in the navigation tree as shown in the figure below.



تصميم و محاكاة هوائي علامة تعريف الموجات الراديوية عالي التردد ثنائي القطب مزدوج

الحث للأجسام المعدنية

إعداد : دالية زاهر منصور

إشراف : د. محمد كوعلي

ملخص :

في الآونة الأخيرة ، نمت تقنية تحديد الترددات الراديوية (RFID) بسرعة في مختلف التطبيقات وخاصة في سلاسل التوريد. تتطلب مثل هذه التطبيقات عددًا كبيرًا من العلامات الموضوعة على أجسام ذات مواد مختلفة بما في ذلك المواد المعدنية التي تزيد من تحديات RFID. يتسبب وجود الأسطح المعدنية في تدهور أداء هوائي علامة RFID. وبالتالي ، يزداد الطلب على هوائيات العلامات المدمجة منخفضة التكلفة وعالية الكسب التي تعمل بفعالية على المعادن .

في هذا العمل ، يتم تقديم هوائي علامة RFID صغير الحجم متبادل مزدوج مطوي ثنائي القطب قابل للتركيب على تردد عالٍ للغاية (UHF). يتكون هوائي علامة RFID المقترح من شريحتين خارجيتين كل منهما محملة بسبعة أذرع مفتوحة متطابقة وشريط متوسط أقصر مكونة أمشاط متناظرة متداخلة . المشطان المتداخلان متصلان في المنتصف بواسطة شريحة RFID التي يتم تثبيتها على القطعتين المتوسطتين . يوفر ضبط أبعاد الدعائم المفتوحة والفجوات بينها آلية ضبط بسيطة ومرنة لتحقيق مطابقة ممانعة مثالية بين هوائي العلامة وشريحة IC عند نطاق تردد التشغيل المطلوب. في الواقع ، توفير تأثير الإقتران (الحث) المتبادل بين الأذرع المفتوحة يزيد من تيار السطح وبالتالي يعزز مجال الإشعاع . تم دراسة تأثير الأذرع المفتوحة عن طريق زيادة عدد الأذرع المضافة من ثلاثة إلى سبعة على كل شريط خارجي. الهيكل المقترح له بعد هندسي $55.8 \times 44 \times 1.5$ مم³ على ركيزة عازلة منخفضة التكلفة من البولي تترافلورو إيثيلين (PTFE). الركيزة مغطاة بطبقة نحاسية رقيقة في الجانب السفلي لتوضع مباشرة على الأجسام المعدنية دون الحاجة إلى أي فاصل مثل الهواء أو الرغوة. تمت محاكاة التصميم باستخدام برنامج CST microwave studio. الكسب المحقق لهوائي العلامة في الفضاء الحر هو -7.13 ديسيبل. أدى وضع هوائي العلامة المقترح على لوح معدني 20×20 سم² إلى تعزيز كسبه المحقق بمقدار 3.57 ديسيبل مقارنة بالمساحة الخالية عند تردد رنين يبلغ 912 ميغاهرتز. حققت مسافة الكشف المحسوبة 11.1 مترًا عند تركيب العلامة على لوح معدني 20×20 سم² و 7.37 مترًا في مساحة خالية مع تقدير استخدام 4 واط EIRP. هوائي العلامة المقترح له اتجاهية تبلغ 3.24 ديسيبل في الفضاء الحر. زادت الاتجاهية إلى 7.36 ديسيبل عند تركيب العلامة على اللوح المعدني. تمت دراسة تأثير تغيير أبعاد الصفيحة المعدنية. يتم تحقيق نفس نطاق القراءة البالغ 11.1 مترًا من خلال تغيير طول اللوح المعدني من 20 سم إلى 10 سم وعرض ثابت يبلغ 20 سم. من ناحية أخرى ، انخفض نطاق القراءة إلى 7.81 مترًا عندما قل عرض اللوحة المعدنية من 20 سم إلى 10 سم بطول ثابت

يبلغ 20 سم. بالإضافة إلى ذلك ، تم وضع هوائي العلامة المقترح على ثلاث ألواح عازلة مختلفة 20×20 سم². الكسب المحقق المحاكي هو -8.63 ديسيبل ومسافة الكشف المحسوبة 6.51 متر عند وضع العلامة المقترحة على لوح من ورق. علاوة على ذلك ، تبلغ مسافة الكشف المحسوبة لهوائي العلامة المقترح 6.29 مترًا و 5.94 مترًا عند وضع العلامة المقترحة على لوح من البولي كربونات 20×20 سم 2 ولوحة زجاجية على التوالي. يتم تنفيذ هوائي العلامة المقدم للعمل في نطاق أمريكا الشمالية (902-928 ميجا هرتز). هيكل العلامة بسيط وغير مكلف ، حيث لا يحتوي على عناصر مختصرة أو معدنية إضافية. لا يتطلب التصميم المقدم أي أعمال تصنيع معقدة . علاوة على ذلك ، فإن علامة RFID المقترحة مضغوطة ولها مكاسب كافية لتحقيق نطاق قراءة مرتفع نسبيًا . وبالتالي ، يمكن استخدام العلامة المقترحة لمختلف تطبيقات RFID .